

## Response to review of manuscript soil-2020-3 by Topical Editor

We would like to thank David Dunkerley for his additional constructive comments to improve the manuscript. The main issues raised by the topical editor are:

- Lack of clear hypothesis stated
- Water content variations with depth should be considered.
- Discussion of hillslope up-scaling should be shortened.
- Stronger emphasis / discussion of Correlation coefficients and PCA in main text.

All of these concerns are addressed in the revised manuscript as explained below in detail. Of particular note, we have added available water content measurements from the study areas, although they are not available in the same spatial fidelity as the pedon geochemical measurements. Further suggested changes are also addressed in the revised manuscript. We hope that our corrections improve the quality of this manuscript in the expected way.

**Thank you for your time!**

**M. Schaller on behalf of all co-authors.**

\*\*\*\*\*

Note: The *topical editor's comments are in italic text*, **our response is in bold text**.

## **Topical Editor Decision: Revision** (05 Sep 2020) by David Dunkerley

*Comments to the Author:*

*Dear Dr Schaller and co-authors,*

*I have read both the reviewer reports and your paper carefully, and have recommended that some moderate revisions be undertaken. Some indication of the areas requiring attention is provided below; I have added some additional comments from my own perspective.*

*The two reviewers have provided some helpful and informative commentary on the manuscript, especially as regards the need to adopt a systematic nomenclature for the weathered materials being discussed. The authors' proposed revisions to the manuscript in light of these comments appear to be entirely appropriate, and should adequately address this issue.*

*Reviewer #2 also commented on the extent to which the work described goes beyond prior published work from the same field sites and using the same GPR methods. All of the soil chemical data analysed in the present paper were derived from prior work at these sites. I therefore think that a fundamental issue to be considered during revision of the manuscript is to make a clear demarcation of what is new and what is derived from prior published studies. For example, in lines 152-155, the paper reports that various soil locations were 'described, sampled, and analysed'. Yet all of this was done*

*in previous studies, not for the current manuscript, as the text may tend to suggest. This needs to be more clearly acknowledged; this is not done until much later (lines 190-191).*

**Sentences in lines 152-155 have been rewritten and clarified. The sentences read now in such a way that it is clear from beginning what is reused and what is new material. “From north to south (Figs 1 and 2), the four selected study areas in the climatic and vegetation gradient observed in the Chilean Coastal Cordillera are: a) Pan de Azúcar (~26.1° S); b) Santa Gracia (~29.8° S); c) La Campana (~33.0° S); and d) Nahuelbuta (~37.8° S). The study areas were investigated for regolith physical and chemical properties by Bernhard et al. (2018) and Oeser et al. (2018) as well as studied with GPR by Dal Bo et al. (2019) (see Tables 1 and 2).”**

*I think that the prior published work could also be cited to avoid the repeated descriptions of methods, since they are in many cases not new. The procedural descriptions make the current manuscript rather long. For instance, in lines 222-22 there is no need to explain what LOI (loss on ignition) means; likewise, I suggest omitting the simple introductory description of GRP in lines 235-240. Readers can either refer to the literature or to a standard text to find this material if they are unfamiliar with GPR methods. Again, I think that you could omit lines 273-285, where the processing of the GPR signals is described, and merely cite the prior published studies from the field sites. At the least, it ought to be possible to greatly abbreviate this material.*

**The method section has been shortened as suggested by the topical editor. The closer description of LOI has been removed (Line 222-224). The chapter 3.2 reads now as: “Ground Penetrating Radar (GPR), a geophysical technique based on the emission of pulsed electromagnetic waves into the subsurface, are applied in this study for frequencies of 500 and 1000 MHz (for more details see Dal Bo et al., 2019). Fourteen new transects going from hillslope toe (near valley) to top (ridge crest) are collected crossing the pedons where physical and chemical properties were collected (Figs. 2 and 3). Of these 14 transects, two were collected in the Pan de Azúcar study area (for 500 and 1000 MHz), six in Santa Gracia (for 500 and 1000 MHz), three in La Campana (for 500 and 1000 MHz), and three in Nahuelbuta (only for 500 MHz). Wide-angle-reflection-refraction (WARR) are used to retrieve velocity and physical properties at the point scale. For each pedon, a WARR is measured in a relatively flat location (red stars, Fig. 2). GPR data were processed and analyzed using MATLAB as described in Dal Bo et al. (2019). In addition, signal envelopes were calculated using a Hilbert transform (Green, 2004; Liu and Marfurt, 2007). At each pedon location, a certain number of traces depending on the measurement step size (i.e. between 10 and 50) were sampled for 0.5 m uphill and 0.5 m downhill the pedon and laterally averaged for comparison to the pedon physical and chemical properties. The averaging assumes that both chemical and GPR signatures do not change with depth**

**across that interval, an assumption that may not hold everywhere. As the GPR envelope is directly related to the electric impedance (Telford et al., 1990; Jol, 2009), the envelope onset and energy intervals could be compared to variations in physical, and potentially chemical, regolith properties.**

*Reviewer #2 also points to a concern over unmeasured water content in the weathered materials examined using GPR. Given that this can strongly influence GPR signals, I think that some further comment is required, especially in light of the likely site-to-site (especially N to S) differences in water content among the sites and at the various depths within the weathered material. In the absence of such data, unknown variation in water content may be confounded with other properties of the materials such as the chemical properties. Presumably, samples for water content determination could readily have been collected in sealed bags for later water content analysis.*

**The pedons described and analyzed in Bernhard et al. (2018) and Oeser et al. (2018) were excavated in early 2016 and promptly refilled due to their locations in national parks and a nature preserve. Unfortunately, water content was not analyzed in pedon samples which were analyzed for the other physical and chemical measures. However, during the 2017 acquisition of the GPR data presented in this study, regolith water content was determined for several auger locations (new Table S3A to C). While these auger samples provide insights into water content variations, they do not exactly spatially coincide with the pedons, and due to the sampling approach (augers) were not sampled at the same depth intervals as in the pedon. Given this – we were not able to include them in the correlation or PCA analysis. However, we do now provide the water content data and refer to it throughout the results and discussion sections. Nevertheless, the available moisture content gives information about the water distribution in space at a given time. Whereas other physical and chemical properties than water content are less time sensitive (e.g., bulk density, clay content) water content changes over days especially in humid areas such as Nahuelbuta.**

*I would like to raise some further issues for consideration, from my own reading of the manuscript.*

*First, I found there to be a lack of clear hypotheses or objectives, though two are listed in the Abstract but not enumerated in the body of the manuscript. Clearly, the study relates to the possible use of GPR methods to extend the available information on soil thickness that can be derived from pit sections. The reasons for seeking to do this are not immediately clear.*

**Aims of this study are incorporated into the introduction. We also now (more explicitly) state the hypothesis tested. With this addition we hope to improve the manuscript and incorporate the editor's suggestion. The introduction finishes now with the following paragraph:** *“In this paper we build upon the previous work of Dal Bo et al. (2019) and compare the pedon measured physical and chemical observations (from Bernhard et al. (2018) and Oeser et al. (2018)) to a large newly acquired GPR data set from the same area to gain insight into regolith variations along a climate and ecological gradient. Our approach is to relate GPR observations adjacent to pedons to depth varying regolith properties caused by weathering as well as to evaluate if these properties can be extrapolated along a hillslope using GPR transects. In doing this, we test the hypothesis that if weathering processes produce depth varying physical and chemical changes in regolith observed in pedons, then (a) GPR based observations of these locations should produce observable changes in the GPR envelope and reflectors correlative to weathering horizons, and (b) GPR can be used to upscale geochemical observations from pedons to the hillslope scale. In general, we find that our new GPR measurements can be correlated to changes in pedolith physical properties if these changes are of sufficient magnitude and laterally coherent. If such a correlation is observed, we discuss the links between the physical and chemical properties. The comparison of physical and chemical properties with field observations and GPR data helps to better understand the regolith at point locations (e.g., pedolith thickness) and in some cases allows for up-scaling point observations to the hillslope scale along a GPR measurement profile.”*

*Moreover, in line 141 (under '2. Study areas', rather than in the Introduction where it would be more appropriate) the manuscript refers to the issue of how climate and vegetation affect soil thickness and GPR observations. This might, for instance, have been listed as an objective in the Introduction. Was investigating this issue indeed an objective of the present work, or not? If it was an objective, then I felt that more information on the site conditions was needed, including for instance NDVI data or some comparable information on the vegetation, perhaps supplemented by aridity indexes, data on seasonality and seasonal variation in climate conditions, and so on.*

**Chapter “2.1 General climate, vegetation, and geologic setting” now includes precipitation and temperature data for the study areas as well as vegetation cover information in the four study areas.**

*In this context, moisture content in the weathered materials would again have been informative. Later in the manuscript, the role of aspect (equator-facing or pole-facing slopes) is raised: was there also an hypothesis underlying this, in light of which the N and S faces were sampled separately? If so, this provides another subject that might be listed in the Introduction as an objective of the current work, if that was indeed the case. Regardless, the reason for sampling both N and S facing sites warrants some explanation, as does the denser sampling of pedon locations on the S-facing slopes than on the N-facing slopes, where only a single site was examined. Readers are likely be interested in the rationale behind such choices.*

**Chapter “5.3 Changes of pedolith thickness with hillslope position, aspect, and latitude” is removed as the closer study of hillslope position, aspect and latitude are not the major objective in this study. The major objective was the comparison of physical and chemical regolith properties with GPR data as well as their up-scaling to hillslopes. Nevertheless, some sentences addressing hillslope position, aspect, and latitude are added to Chapter 5.2 in order to state that the observations from this study are comparable with Bernhard et al. (2018) and Dal Bo et al. (2019).**

*In relation to the field sites, I noted that the hillslope study sections are in some cases extremely short: apparently < 3 m in the N-facing site at Nahuelbuta, to judge from Figure 3. Extrapolation from the pedon to the hillslope scale over a distance of < 3 m amounts to only a very limited extension of the pedon data. Similarly, the S-facing slope at Pan de Azucar appears to be < 10 m long, raising similar issues. In general, I think that some additional commentary on the scale of the topography being studied would be helpful for readers. For instance, is the challenge of extrapolating from pedon to hillslope over such short hillslopes typical of the challenge faced more generally in such work? In other words, do these sites constitute an informative test case?*

**In order to avoid questions such as raised by the topical editor, the following text is added to the manuscript in Chapter “2.2 Regolith characteristics”: “Only one pedon was investigated in the N-facing slopes due to time and financial restrictions. In addition, transect lengths in some settings are limited due to the availability of weathered hillslopes in the same lithologies (e.g., Pan de Azucar; Fig. 3A) as well as restriction of access due to intense vegetation (e.g., Nahuelbuta; Fig., 3D).”**

*The manuscript touches on hillslope aspect and its relationship to soil thickness (lines 622-624). Here I felt that if this topic is to be discussed, then wider acknowledgment of the growing published literature on this topic was needed. I mention here a few studies that came to mind only as examples. The literature on this topic is now quite large.*

*Yetemen, O., E. Istanbuluoglu, J. H. Flores-Cervantes, E. R. Vivoni, and R. L. Bras (2015), Ecohydrologic role of solar radiation on landscape evolution, Water Resour. Res., 51, 1127–1157, doi:10.1002/2014WR016169.*

*Yetemen, O., E. Istanbuluoglu, and A. R. Duvall (2015), Solar radiation as a global driver of hillslope asymmetry: Insights from an ecogeomorphic landscape evolution model, Water Resour. Res., 51, 9843–9861, doi:10.1002/2015WR017103.*

*Srivastava, A. et al. (2019). Aspect-controlled spatial and temporal soil moisture patterns across three different latitudes. 23rd International Congress on Modelling and Simulation, Canberra, ACT, Australia, 1 to 6 December 2019*

[mssanz.org.au/modsim2019](http://mssanz.org.au/modsim2019).

*Inbar, A. et al. (2018). Climate dictates magnitude of asymmetry in soil depth and hillslope gradient. Geophysical Research Letters 45, 6514-6522.*

**Chapter 5.3 discussing hillslope position, aspect, and latitude, is removed and replaced by a short section in Chapter 5.2. Therefore, we do not incorporate all the suggested references. The removal of Chapter 5.3 not only shortens the already long paper but hopefully also helps to improve the focus of this paper.**

*In the Discussion section, I think that there is much speculative material that would likewise benefit from additional supporting references. For example, there is the unreferenced claim that*

*"From the top- to toe-slope position along a catena the potential for physical erosion decreases downslope due to decreasing physical potential whereas the potential for deposition increases".*

*There are certainly many situations where this does not apply; in drier climates the volume of overland flow may increase downslope, and whilst hillslope gradients might decrease there, the surface roughness may decline such that the surface runoff becomes faster and more erosive. Rilling and gullying are consequently often characteristic of footslopes, not the steeper upper slopes. The more general point is that, in order to interpret soil thickness and the variables that influence it, some knowledge of the erosional and geomorphic processes that operate at the site concerned is really needed. None is provided in the current manuscript, and it would be helpful if something could be said. Similarly, in discussing the different patterns of soil thickness on N and S-facing slopes (lines 624-642) the manuscript is almost entirely speculative. The authors hypothesise that some differences might perhaps relate to aspect-related differences in soil moisture (lines 624-625) or vegetation cover (line 627) or subtle lithological changes (line 630) or local heterogeneities in erosion (lines 634-635) or even other processes such as differences in evaporation (line 641). Given that the manuscript presents no evidence bearing on these issues, I think that this discussion might be curtailed somewhat. Reference to prior published work on this topic (see suggestions above) would support some brief comments. The authors also raise some issues in passing, that are not given further attention in the manuscript. For instance, they mention possible site-to-site differences in bedrock joint spacing (line 165), but do not discuss how important such variation might be in affecting their results. In this context, I was conscious of the recent work of Leone et al. (reference below) in Arizona where regolith thickness was influenced not primarily by aspect but by the orientation of the foliation in the underlying bedrock, in relation to the topography. This is an instance that reminds us that weathering and soil production can be influenced by much more than surface climate, vegetation, or three-dimensional hillslope curvature.*

*Leone JD, et al. (2020). Strong slope-aspect control of regolith thickness by bedrock foliation. Earth Surface Processes and Landforms. Available in Early View.*

**As explained above Chapter 5.3 has been removed and replaced with a paragraph in Chapter 5.2. The speculative material does not need more discussion nor more references. This rearrangement should shorten and clarify this manuscript.**

*Finally, I think that the Pearson correlation analysis that is set out in section 3.3 ('statistical correlation and principal components analysis') is poorly utilised in the paper. This is suggested as one of the new contributions of the manuscript (lines 37-39). No correlations are actually presented in the paper; rather, these are only briefly qualitatively referred to, and the actual data are relegated to the Supplementary information. Little appears to be said about the correlations, and therefore perhaps the long methods description relating to this work (lines 296-311) could be abbreviated. Alternatively, if the correlations are regarded as important, then perhaps more analysis of these results could be incorporated.*

**The discussion of the reported correlations for the four study areas and the entire Earth Shape climate and vegetation transect is extended. Therefore, the previous Table S3 with the correlation information is now moved to the main text as suggested. The main text contains now 3 Tables. The method section is shortened.**

## Response to review of manuscript soil-2020-3 by RC1

### Preface to the response to reviews by the authors:

We would like to thank Colin Pain for his constructive comments to improve the manuscript. The regolith terminology has been adjusted to World Reference Base for Soil Resources (WRB). This adjustment should clarify some of the confusion created. Furthermore, all of the following changes we've made to the manuscript have been implemented in the manuscript text file.

Note: The *reviewer's comments are in italic text*, **our response is in bold text**.

Thank you for your time,

**M. Schaller on behalf of all co-authors.**

\*\*\*\*\*

### General comments

*This paper reports on correlations between GPR profile data and physical and chemical soil properties. The soil properties come from work that has previously been published, while the GPR data are new. The correlations are discussed and demonstrate that GPR can be used to infer soil thicknesses and to a lesser extent soil properties. The paper is well written and is a very useful contribution to our knowledge of the value of using geophysical methods to study soil properties and distribution. I suggest a change to the title: "Comparison of regolith physical and chemical characteristics with geophysical data along a climate and ecological gradient, Chilean Coastal Cordillera (26° to 38° S)".*

**Line 1-3: The title has been changed as suggested by the referee. Only soil has been replaced by regolith to be consistent with the rest of the manuscript and reviewer comments.**

### Specific comments

*There is some confusion in soil/regolith terminology. Regosol, cambisol, and umbrisol are World Reference Base for Soil Resources (WRB) classes. I think it would be useful to mention this, and to briefly discuss the soil classification. Part of the confusion is the distinction between soil and saprolite – the saprolite is the C horizon and is therefore part of the soil. While there is clearly a difference between the mobile zone (A and B horizons) and the underlying saprolite zone (C horizon), both are parts of the soil profile. (The mobile zone may be transported by creep or surface wash, or it may simply be re-sorted, as by termites or earthworms, or it may be a combination of both, so it is a very general term.) For this reason, I disagree with Riebe and Granger (2013) when they restrict the term "soil" to the mobile zone.*

**The terminology of used in this manuscript has been adjusted to "World Reference Base for Soil Resources".**

## Response to review of manuscript soil-2020-3 by RC2

Summary of revisions made for the benefit of the Editor, and reviewer:

We thank the reviewer for the time she spent reviewing this manuscript, although the tone of many of the comments was unnecessary. This reviewer's comments are in stark contrast to the positive and constructive comments of the first reviewer. Nevertheless, we've tried our best to address this reviewer's concerns. The reviewer's comments revolve around:

- a) Not clearly understanding the differences in data and analysis presented between our previous study (Dal Bo et al., 2019) and this one.
- b) Suggesting many changes for this paper to have a different scope than what we state are our aims in the introduction.
- c) Continually emphasizing the importance of moisture data (which is not available), while many other difficult to acquire geochemical data sets are compared to extensive new GPR data with a multivariate analysis.

To address these items, we have modified the text to more explicitly state the differences between our previous work and this study, and to highlight more prominently caveats associated with this study – such as no regolith moisture data availability. We note, however, that although this reviewer comments on the need for additional referencing of “gray” literature, no references (peer reviewed or otherwise) were provided in their entire review.

Finally, we honestly struggled in many places to understand what the reviewer was trying to say in her comments below and edits to the manuscript text. The edited manuscript she provided also changed text in many places to be grammatically incorrect (e.g. removal of the verb in a sentence, or incorrect preposition use, etc), and more confusing. We've tried to implement all these changes as best we could, and highlight below where we disagree with the reviewer's strong opinions for what the study should be.

**Note:** The *reviewer's comments are in italic text*, our response is in bold text.

Thank you for your time,  
M. Schaller on behalf of all co-authors.

\*\*\*\*\*

### General comments

*This paper is a somewhat disappointing addition to work already published by the team working on the German-Chilean priority research program EarthShape ([www.earthshape.net](http://www.earthshape.net)). The published work has already established that GPR could be used to map “soil” materials in the four study areas, and that interpretation can be “up scaled” from point observations to transects (Dal Bo et al. 2019). The Dal Bo et al. paper correctly identifies the importance of observations about soil moisture content and clay content to refinement of GPR data interpretation. Note, increases in both soil*

*moisture and clay content often mark the transition from pedolith to saprolith. Unfortunately, Schaller et al. do not expand on the soil property dataset already available to Dal Bo et al., and so, unsurprisingly, do not come up with any new insights into the interpretation of their new - or the old (Dal Bo et al.) - GPR data acquired in the EarthShape Chilean study areas.*

**With all due respect, we disagree with the reviewer's assessment of our previous work and this manuscript. The following items were stated in the manuscript, although we've modified the text (sections 1 (introduction) and 5.2 (discussion) to make this clearer for other reviewers. More specifically, our disagreement with the reviewer stems from:**

- **There is NO overlap in GPR or regolith property data presented in this manuscript or the Dal Bo et al., 2019 manuscript. Entirely new GPR profiles are presented here. Dal Bo et al. (2019) only use the observed transitions from B-C horizons in Bernhard et al. (2018), and the boundary between mobile and immobile layer from Oeser et al. (2019).**
- **At the time the Dal Bo et al. (2019) manuscript was prepared in February 2018, the physical and chemical properties of the regolith used in this (current) SOIL journal manuscript were not available for use. This is in part to our honoring of Bernhard et al. (2018) and Oeser et al. (2018), having the right to publish their data first, and also due to extremely long editorial handling (~1.5 years) of the Dal Bo et al. (2019) in CATENA.**
- **Thus, these regolith property data were not available to use in our 2019 study as the review suggests and there is no duplication of regolith property data. In fact, the scope of the Dal Bo et al. (2019) study and this manuscript are different and we are perplexed why the reviewer is criticizing a previously published study for not including additional data. This simply wasn't possible.**
- **The focus of Dal Bo et al. (2019) is on identifying the boundary between the pedolith and saprolite. This is a very different scope than the current (Schaller et al.,) manuscript in the journal SOIL where the focus is on comparison to a large number of chemical and physical property data.**
- **In contrast, this manuscript (Schaller et al.) tries to correlate the observed signal with physical and chemical changes provided by Bernhard et al. (2018) and Oeser et al. (2018). This is the logical next step for a study where there are co-located and potentially complementary data sets.**
- **Finally, it is true that envelopes of the GPR signal are already presented in Dal Bo et al. (2019) although these envelopes come from a different data set, and slightly different geographic positions such that a robust comparison to pedons was not possible. In contrast, this manuscript by Schaller et al. correlates the envelope intensity with physical and chemical changes. This in turn allowed a more quantitative determination of the pedolith depth over a hillslope transect.**
- **Concerning clay and water content variations in our study area – we address this comment below. In short, clay content variations are**

accounted for in our PCA analysis, whereas water content variations have not been measured and are not available for study.

In summary, while we strongly disagree with the reviewer's statements concerning our previous work, we take their comment to highlight that the manuscript could provide a clearer distinction to our previous work. Given this, we have expanded the introduction to more explicitly state the differences with previous work.

*I would suggest that the authors, and the EarthShape team, take a closer look at some of the work that is being done on using GPR to map regolith materials and processes elsewhere in the southern hemisphere, especially in Australia. Some of this work is published in "grey" literature, but it is still relatively easy to find on the internet. There is also a lot of work being done in Australia, some in collaboration with European geophysicists, on the use of electromagnetic surveys to map regolith materials and processes. The inversion of this data has become quite sophisticated and AEM surveys, designed in part to map regolith thickness, are now taking place on a continental scale.*

The EGU SOIL journal guide for authors states (<https://www.soil-journal.net/submission.html#references> ) states that "Grey" literature should not be cited, specifically: *"Informal or so-called "grey" literature may only be referred to if there is no alternative from the formal literature. Works cited in a manuscript should be accepted for publication or published already"*. In our manuscript, we cite related published literature so citation of 'Grey' literature is not needed. Furthermore, the reviewer's request to cite other 'southern hemisphere, especially in Australia' studies was not accompanied with specific references to consider. We've conducted literature searches to see what other relevant literature could be cited, but without specific recommendations from the reviewer we cannot accommodate this statement, nor will we cite grey literature as this is not commonly accepted for high-quality peer review journals (such as this one).

*Further, Schaller et al. perpetuate some of the confusion in soil and regolith terminology that is apparent in earlier work by this team. In particular, the confusion relates to the use of the term "soil" variously as a descriptor for the entire regolith profile (pedolith and saprolith), and as a descriptor solely for the pedolith. This confusion is exacerbated by reference to soil materials that are mobile (pedolith) and immobile (saprolith). Note, the saprolith includes saprolite and saprock.*

Reviewer 1 had a similar comment. There is a difference in terminology between the surface processes and soils communities, and we had provided a reference for the terminology we were following. However, given that this journal is a soil sciences community journal, we have adjusted the terminology as requested. The terminology of soil used in this manuscript has been adjusted to "World Reference Base for Soil Resources" as suggested by reviewer 1.

*The distinction between these units can be important for the interpretation of geophysical data, although the EarthShape Chilean study does not appear to have properly investigated beyond the pedolith. A visit to some of Chile's open cut mines might be a salutary experience in this regard.*

**We thank the reviewer for this suggestion, but in practicality, we are not sure how this would be useful at this time. In particular,**

- **The investigation of the pedolith is the main topic of this manuscript and much of the EarthShape Phase 1 research. Several months ago other EarthShape projects completed drill cores within about 10 km of each study area to study saprolite, saprock, and bedrock. What we learned is that the bedrock is hard to reach and is reached at ~30 to ~80 m depth. These drill cores and data from them are still 1-2 years away from publication (at the earliest) and are not available for this study.**
- **We are not sure what insights the proper investigation beyond the pedolith in an open cut mine would change the interpretations made in this study, particularly because they would be located far off site from the actual study area where physical and chemical measurements were made and lateral extrapolations from regolith formed in different host lithologies where we have no chemical or physical measurements would not provide a robust comparison.**

*Note, these general comments are supplemented with detailed comments and suggested amendments as per the attached pdf. The comments and suggested amendments have been added to the pdf using Adobe Acrobat.*

**Detailed comments and changes are addressed below in supplemental comments.**

### **Supplement comments**

*Please also note the supplement to this comment:*

*<https://soil.copernicus.org/preprints/soil-2020-33/soil-2020-33-RC2-supplement.pdf>*

*Line 48-52:*

*"Pedolith" may be a better term than "soil" with reference to a regolith profile*

*"Saprolith " may be a better term than "saprolite" with reference to a regolith profile esp as saprolith includes both saprolite and saprock*

*"Meaningless sentence in this context, as the saprolith is, by definition, immobile. It is only after it's weathering products engage with biological and hydrological processes that they "enrich" the pedolith"*

**The use of soil for the mobile layer is replaced by the term pedolith. The entire manuscript has been checked for consistent use. Also, the remaining regolith**

terminology has been adjusted to “World Reference Base for Soil Resources” as suggested by Reviewer 1. The sentence reads now the following: “Most biota is found in the mobile pedolith, which overlies the immobile saprolith. The pedolith is replenished with nutrients from the saprolith through chemical weathering and erosion that drives nutrient uplift towards the surface (e.g., Porder et al., 2007).

*Line 52-54:*

*This list of factors does not follow a logical sequence and as such is confusing. In my view the list should progress from the local to the regional. Aspect, which is highlighted in proceeding published work, has been omitted altogether.*

*Regolith thickness or "soil" thickness?? Having started with regolith I think it is best to stick with regolith.*

The sequence of the list has been adjusted as suggested by referee 2. Aspect is added as a factor. The term “soil” is not used anymore. The investigated depth sequence is named “regolith” and the so far named “soil” is relabeled “pedolith”. The sentence reads now as follows: “The thickness and production of regolith is influenced by aspect, topography, composition (mineral content), biota, climate, tectonically driven rock uplift, and time (e.g., Hilgard, 1914; Jenny, 1994).

*Line 55-56:*

*Regolith thickness or "soil" thickness?? Having started with regolith I think it is best to stick with regolith.*

The sentence reads now as follows: “However, sub-surface variations in pedolith thickness at the scale of hillslopes are difficult to quantify because of lack of exposure.”

*Line 56-59:*

*See previous comment and ditto for all references to "soil" in this section*

The use of regolith terminology has been adjusted as suggested by the referee in the entire manuscript. The sentence reads now as follows: “Thus, subsurface imaging by geophysical techniques, when calibrated to regolith excavations (pedons), offers potential to characterize spatial variability in pedolith thickness and regolith properties (e.g., Mellett, 1995; Doolittle and Collins, 1995; Miller et al., 2004).

*Line 83-85:*

*However, on a theoretical basis, the importance of certain properties has been identified eg soil moisture content and clay content cf proceeding work by this team published in Dal Bo et al 2019.*

**Not sure we understand what change the reviewer is asking for. The sentence reads now: “Interpreting the interplay of GPR signals with physical and chemical regolith properties is challenging (e.g., Saarenketo, 1999; Sucre et al., 2011; Tosti et al., 2013; Sarkar et al., 2019).”**

*Line 89-92:*

*Biotic processes are "critical zone" or more properly "regolith" processes*

**The term ‘critical zone’ is replaced by “regolith”.**

**“The region is home to four study areas of the German-Chilean EarthShape priority program ([www.earthshape.net](http://www.earthshape.net)), where investigations of biotic interactions with regolith are conducted (e.g., Bernhard et al., 2018; Oeser et al., 2018).”**

*Line 141:*

**Soil has been replaced by pedolith: “To compare the effect of climate and vegetation on pedolith thickness and GPR observations, differences in lithologies need to be minimal.**

*Line 158-161:*

*a saprolith (which includes saprolite and saprock and thus includes the "C horizon"*

**The sentence has been changed to: “In this study, we refer to depth profiles as regolith profiles that are composed of a mobile pedolith that includes the A and B horizons, and an immobile saprolith including the C horizon.”**

*Line 162-163:*

*Alternatively "has been described as"*

*WRB ref needed*

**The sentence has been corrected as suggested by referee 1 and reads like:’ In Pan de Azúcar, the regolith, a regosol (IUSS Working Group WRB, 2015), consists of A and B horizons with a combined thickness of 20 to 25 cm and an underlying saprolith (the C horizon), which is coarse-grained and jointed (Oeser et al., 2018). The requested reference has been added.**

*Line 165-166:*

*The entire regolith profile ie pedolith and saprolith or just the pedolith??*

The sentence has been corrected to: “The average bulk density of the A and B horizons is 1.3 g cm<sup>-3</sup>.”.

*Line 166-168:*

“The cambisol in Santa Gracia consists of 30 to 55 cm thick layers of soil with A and B horizons overlying the saprolite (Bernhard et al., 2018).” The sentence has been changed to: “In Santa Gracia, the 30 to 55 cm thick pedolith overlying the saprolith is a cambisol (Bernhard et al., 2018).”

*Line 234:*

*As previously noted, both the physics of GPR data acquisition and work carried out elsewhere suggests the importance of soil moisture content. Why wasn't data on this property acquired?*

**We agree with the reviewer that regolith moisture content is important and would be nice to know. Unfortunately, this data is not available. The pedons that we compare our GPR data to were excavated in March 2016, and promptly filled in by July 2016 because they were located in national parts. Regolith moisture measurements were not made on samples collected in 2016, and no pedons were available for sampling at the time the GPR data for this manuscript was collected in 2017. Furthermore, as the reviewer likely knows, regolith moisture varies both seasonally and annually, such that comparison to regolith water content measurements from a previous year would be difficult to assess the robustness of.**

**To address this reviewer’s comment – we have modified the text (Section 3.1 methods/data compilation) to also state more clearly that regolith moisture is important (amongst other factors) for GPR data interpretation, but that this data is not available. We had already mentioned this in the text, but we make it clearer now to hopefully reach a happy middle ground with this reviewer. We also address this topic in the new concluding discussion section 5.4.**

**Furthermore, we addressed this topic, and other limitations / caveats of the study, in a new concluding discussion section “5.4 Comparison to previous work and study caveats”. Hopefully this reaches a happy middle ground with the reviewers concern.**

**Finally, clay content is also important for GPR data interpretation (as the reviewer mentioned earlier). We note that clay content was measured and reported by Bernhard et al. (2018), and we have included this in our PCA analysis.**

*Line 344-346:*

*pedolith/saprolith*

**“Mobile/immobile” has been changed in the entire manuscript “mobile and immobile” as suggested by referee 1. The terminology “pedolith/saprolith” is not used because Oeser et al. (2018) used the terms “mobile/immobile” for the boundary they observed. The sentence reads as follows: “In Pan de Azúcar (Fig.1, 2A), a gradual transition from the B to the C horizon was visually observed in the pedons at 20 to 40 cm (shaded gray areas after Bernhard et al., (2018); Fig. 4, Fig. S1 to S3), whereas the mobile and immobile boundary is considered to be at 20 to 25 cm (black lines after Oeser et al., (2018); ); Fig. 4, Fig. S1 to S3).**

*Line 390:*

*pedolith/saprolith*

**See response above for line 344-346.**

*Line 385-387:*

*pedolith/saprolith*

**See response above for line 344-346.**

*Line 387-390:*

*?pedolith*

*? pedolith or total regolith*

**Sentence reads now as: “Bulk density and grain size change gradually with depth and no clear pedolith thickness could be determined.”.**

*Line 409:*

*pedolith/saprolith*

**See response above for line 344-346.**

*Line 416:*

*pedolith/saprolith*

**See response above for line 344-346.**

*5.1 Synthesis of GPR data with physical and chemical properties from point locations*

*Suggest that theory and the findings of previous studies throughout the world should be the starting point ie properties such as soil moisture content, salinity and clay content, should be the starting point for this discussion. Some of the measured properties could be considered proxies for these properties of known importance, and the discussion should be explicit in that regard.*

**We thank the reviewer for this comment. We agree that more general discussion of factors influencing GPR data could be discussed. However, we did not include this in section 5.1 because this section focuses on synthesizing our results and interpreting them. However, to accommodate the reviewers concern, we have added a new section 5.4. We hope that this addition improves the manuscript further.**

*Line 443:*

*Soil moisture content is known to be important so why has this been neglected in this study?*

**Please see our response to this reviewer’s comment for line 234 above. The data is not available! However, we’d like to emphasize that while regolith moisture content would be nice to have for inclusion into our PCA analysis, the lack of having this data does not invalidate the observations we present. The addition of this data would help constrain the interpretations better, but it’s not available. We expanded text related to regolith moisture in section 3.1, and 5.4.**

*Line 448:*

*Was "basal saturation" as reported by et al 2019 useful? If not, why not?*

**We apologize, but we do not understand what the reviewer is referring to here. We conducted a “find” on the manuscript text and do not see the word “basal saturation” used by us. The same words do not appear in the work of Dal Bo et al. (2019). Also – we are unclear why the reviewer is commenting on a previous (published) study whose data are different from this study, and not collected in the same location.**

*Line 449:*

*? pedolith/saprolith*

**Sentence has been changed by referee 1 and reads now as: “In addition, the determination of the boundary between the pedolith and saprolith in the field causes its own problems because observed changes are not discrete but transitional over a depth interval of 5 to 10 cm”.**

*Line 457-459:  
? within the saprolith*

**Sentence has been changed: "Whereas the 500 MHz signal shows interfaces in the saprolith, the maximum in the 1000 MHz energy interval signal agrees with the pedolith thicknesses observed in the field (Fig. 4 and Figs S1 to S3)."**

*Line 459-461:  
? pedolith and saprolith*

**Sentence has been changed: "However, the boundary between pedolith and saprolith is probably too shallow to be detected with the 1000 MHz antennae."**

*Line 461-462:  
? pedolith and saprolith*

**Sentence has been changed: "An even higher frequency would be required to detect the pedolith/saprolith boundary."**

*Line 473:  
Theory would suggest that in such shallow dry and uniformly sandy "soils" GPR might be useful in mapping changes in moisture content over time*

**We don't disagree with the reviewer that GPR data are also sensitive to regolith moisture, but we don't understand what the reviewer is asking for in this comment.**

*Line 474-478:  
Does this mean that the visual observations are not supported by physical and chemical measurements?*

**Correct. The sentence reads as: "Although the 500 MHz and 1000 MHz GPR envelopes indicate changes at depth, the physical and chemical properties observed with depth show only a few distinct changes implying that the pedolith thickness cannot easily be determined using only physical or chemical properties."**

*Line 486-488:  
Well known, which is why forward modeling of "remote" geophysical data should be supported by the best available petrophysical data*

**Sentence changed to: “These observations again underscore, that for different locations with variable regolith type, vegetation, and physical and chemical properties local calibration between pedons and GPR data are required.” Forward modeling of GPR data is not the stated intent of this manuscript, and is beyond the scope of this study. This manuscript focuses on comparisons between geochemical and geophysical data, not forward modeling of geophysical data.**

*Line 497-498:*

*Is this a consequence of an increase moisture levels?*

“Chemical properties seem to have a considerable influence on GPR signals in this setting”

**We are unclear as to what the reviewer is asking for here. Regolith moisture was not available for comparison. What the PCA analysis tells us is the variables that co-vary with each other. Any other variables not included in the PCA analysis (e.g. moisture levels) would be lumped into the unexplained variance in the analysis. If regolith moisture co-varies with the chemical properties measured, then it would also show up in the analysis. However, we are not aware of any published work that shows co-variation of regolith moisture with the chemical properties measured here. As such, we do not see a basis for adding speculation on this here.**

*Line 505:*

*The most important of which are?*

**Physical properties have been listed. The sentence reads now as: “The pedolith thickness is easily identifiable based on physical properties (e.g., bulk density, grain size variation).”**

*Line 508-510:*

*Related properties*

**We are not sure what properties the reviewer is asking for here since we already mention relevant properties we can constrain. The sentence reads: “The variance is strongly explained by PC1 containing physical properties (e.g., bulk density, clay content, LOI) and less by PC2 including chemical properties (e.g., pH,  $\tau$  of Na and Zr).**

*Line 545-547:*

*How do these results compare with those reported by Dal Bo et al 2019?*

Figures 12 to 15 and figures S14 to S23 show the pedolith thickness based on visual observations in the GPR signal as well as the pedolith thickness based on amplitude signal in the GPR envelope signal. The pedolith thickness determined by the GPR signal generally agrees with the pedolith thickness based on GPR envelopes. However, pedolith thickness based on GPR signals is not always possible, GPR envelopes give continuous information where a change from pedolith to saprolith is to be expected. The sentence in questions is changed to: “However, the complications which frequency of GPR antenna to use for analysis (Dal Bo et al., 2019) in addition to what envelope interval to select (section 5.1) requires careful up-scaling of the pedolith thickness to hillslopes.”

*Line 557-559:  
? down*

**Sentence corrected as suggested: “The pedolith thickness based on the 1000 MHz GPR envelope at the top-slope position (SGPED20) decreases first downhill and then increases again, thereby demonstrating laterally variability down the hillslope.”**

*5.3 Changes of soil thickness with hillslope position, aspect, and latitude  
This topic is thoroughly explored in preceding publications by this group*

**Yes, we know we’ve written about this topic before. We address it again here because a lot of new (and different types) of data are presented and it is important point for the community to know if the previous results still stand. Furthermore, the study areas presented in here were specifically chosen to address variations due to hillslope position and latitude and we’d be remiss not to cover this.**

*Line 660-662:  
?pedolith to saprolith  
Although the correlations are not consistent from one area to the next*

**Sentence corrected: “The visually observed transition from the mobile pedolith to immobile saprolith coincides with one or more changes in measured physical and chemical properties in each study area.”**

*Line 662-665:  
This could be because the data on "soil" properties did not include data on properties known to be an important influence on GPR responses eg soil moisture content. As a consequence, the work could be considered to be inherently flawed.*

**The way in which this comment is worded is unnecessarily offensive. Nevertheless, we don't disagree that regolith moisture can also be important. As stated before, regolith moisture data was not available. However, many other relevant data sets were available and a multivariate analysis was conducted to identify where signals do lie within the data. In some cases - a large amount of variance in the data set is explained by these data. In other cases not. In the cases where all the variance is not explained, yes – this could be due to other factors like regolith moisture.**

**To address this comment, we have modified the text in section 3.1, and also in the new 'caveats' section in the discussion section (section 5.4) to more explicitly state these caveats and the other factors (such as regolith moisture) could also be important for observed GPR signals.**

**To say the study is inherently flawed when a comparison of GPR data to difficult to acquire chemical data is frankly surprising. There are very few studies to our knowledge that conduct this detailed comparison between chemical and geophysical data over a ~1300 km ecological and climate gradient in a similar lithology. We apologize if the reviewer doesn't see the merits in this. Reviewer 1 did explicitly recognize the utility of this.**

*Line 6742-674:*

*Not new findings. Petrophysical data, or an understanding of the variation in the properties being investigated at a local scale, are fundamental to proper design, processing and interpretation of all geophysical surveys.*

**Yes – we are aware that the GPR community frequently conducts subsurface point calibrations to their data. The sentence the reviewer is referring to here is the last sentence of the conclusions and is a wrap up sentence. We've deleted the sentence for the reviewer's benefit. We've added a new concluding sentence to this section that gives more details about what frequency antennas work better in which climate/vegetation zones.**

*I would find photos of the soil/saprolite profiles useful. Perhaps you could include photos and soil profile descriptions in the supplementary file? Or refer to Figure 2 in Bernhard et al (2018) – perhaps even reproduce it. It is a very useful figure and should be easily available to readers of this paper.*

**We thank the reviewer for this suggestion. We prefer not to republish figures from other figures, but to accommodate this suggestion we have add reference in the main text (section 2.2) and the figure caption for our Figure 3 to say: (for complete characterization and interpretation of the pedons see Fig. 2 in Bernhard et al. (2018) and Figs 3 to 6 in Oeser et al. (2018)).**

*Lines 162 and 163. “In Pan de Azúcar, the soil is part of a regosol and consists of a 20 to 25 cm thick A and B horizon.” A regosol is a soil, so how can the soil be part of it? I suggest rewording: “In Pan de Azúcar, the soil, a regosol, consists of A and B horizons with a combined thickness of 20 to 25 cm and an underlying saprolite zone (the C horizon), which is coarse-grained and jointed (Oeser et al., 2018). The total organic carbon content of the A and B horizons is <0.1% (Bernhard et la., 2018). Angular fragments in the soil increase in size (> 1 mm) with depth.”*

**Sentences have been reworded as suggested: “In Pan de Azúcar, the regolith, a regosol, consists of A and B horizons with a combined thickness of 20 to 25 cm and an underlying saprolith (the C horizon), which is coarse-grained and jointed (Oeser et al., 2018). The total organic carbon content of the A and B horizons is <0.1% (Bernhard et la., 2018). Angular fragments in the pedolith increase in size (> 1 mm) with depth.”**

*I also suggest rewording soil descriptions for the other areas in the same section. Soil descriptions have been adjusted in all sections to terminology used in first section.*

*Section 2.2. For La Campana and Nahuelbuta there is no mention of the characteristics of the saprolite.*

**For Santa Gracia, La Campana, and Nahuelbuta the saprolith is now mentioned and shortly described in section 2.2.**

### **Technical corrections**

*Line 88. What do you mean by “sub-surface”?*

**“sub-surface” has been changed to “regolith” where not used in connection with GPR analysis.**

*Figure 3 caption – what do the colours in the pedons represent?*

**A legend for the colors used in this figure has been added to the figure.**

*Line 254, also 278 “In this way, the move-outs of linear events” – I/m not sure what this means – what are “move-outs”?*

**The sentence with the term “move-outs” has been replaced by: “Using this type of survey, we can distinguish between signals that increase linearly in traveltime with increasing receiver-transmitter distance (e.g., air wave and ground wave) and signals that increase hyperbolically in traveltime with increasing receiver-transmitter distance (e.g., subsurface reflections). In this analysis, we assume that internal reflection horizons are not dipping.**

*Check figures for text size. In some (e.g. Figure 4, Figure 6, some of the text is too small. I attach a file with suggested edits.*

**Figure 4, 6, 8, and 10: Font sizes have been enlarged where possible. The same changes have been applied on the supplementary figures in question.**

#### **Additional comments**

*This is not a comment on your paper, but a general comment on the research. Have you considered using ground-based electromagnetic sensing? This measures conductivity and might supplement GPR as a way of mapping sub-surface soil units. See, for example: Ahmed, M.F., Odeh, I.O.A. and Triantafyllis, J. 2002. Application of a mobile electromagnetic sensing system (MESS) to assess cause and management of soil salinization in an irrigated cotton- growing field. *Soil Use and Management* 18, 330-339. Triantafyllis, J. and Buchanan, S.M. 2009. Identifying common near-surface and subsurface stratigraphic units using EM34 signal data and fuzzy k-means analysis in the Darling River valley. *Australian Journal of Earth Sciences* 56, 535-558. Amezketa, E. 2007. Use of an electromagnetic technique to determine sodicity in saline - sodic soils. *Soil Use and Management* 23, 278-285.*

**Unfortunately, electromagnetic induction EMI was applied, but did not produce reliable results. Therefore, EMI analyses were not included in Dal Bo et al. (2019) and did not get measured in the second field campaign performed for this manuscript. Thank you for this suggestion and the references addressing this kind of investigations.**

#### **Supplement comments**

*Please also note the supplement to this comment:*

*<https://soil.copernicus.org/preprints/soil-2020-33/soil-2020-33-RC1-supplement.pdf>*

**All suggested changes have been taken into account in the manuscript.**

1 **Comparison of regolith physical and chemical characteristics with**  
2 **geophysical data along a climate and ecological gradient, Chilean Coastal**  
3 **Cordillera (26° to 38° S)**

Deleted: soil

Deleted: from

Deleted: and geochemical techniques

4  
5 Mirjam Schaller<sup>1\*</sup>  
6 Igor Dal Bo<sup>2\*</sup>  
7 Todd A. Ehlers<sup>1</sup>  
8 Anja Klotzsche<sup>2</sup>  
9 Reinhard Drews<sup>1</sup>

10 Juan Pablo Fuentes Espoz<sup>3</sup>  
11 Jan van der Kruk<sup>2</sup>

12

13 <sup>1</sup> Department of Geosciences, University of Tübingen, Schnarrenbergstrasse 94-  
14 96, 72076 Tübingen, Germany

Deleted: Germany,

15 <sup>2</sup> Agrosphere (IBG-3), Institute of Bio- and Geosciences, Forschungszentrum  
16 Jülich, 52428, Jülich, Germany

17 <sup>3</sup> University of Chile, Department of Silviculture and Nature Conservation, Av.  
18 Santa Rosa 11315, La Pintana, Santiago RM, Chile

19 \* Authors contributed equally.

20

21 Corresponding author: E-mail: Mirjam Schaller (mirjam.schaller@uni-  
22 tuebingen.de)

23

24

29 **Abstract**

30 We combine geophysical observations from Ground Penetrating Radar (GPR)  
31 with regolith physical, and chemical properties from pedons excavated in four study  
32 areas spanning 1,300 km of the climate and ecological gradient in the Chilean  
33 Coastal Cordillera. Our aims are to: (1) relate GPR observations to depth varying  
34 regolith physical and weathering-related chemical properties in adjacent pedons,  
35 and (2) evaluate the lateral extent to which these properties can be extrapolated  
36 along a hillslope using GPR observations. Physical observations considered include  
37 regolith bulk density and grain size distribution, whereas chemical observations are  
38 based on major and trace element analysis. Results indicate that visually-  
39 determined pedolith thickness and the transition from the B to C horizons generally  
40 correlate with maximums in the 500 and 1000 MHz GPR envelope profiles. To a  
41 lesser degree, these maximums in the GPR envelope profiles agree with maximums  
42 in weathering related indices such as the Chemical Index of Alteration (CIA) and the  
43 chemical index of mass transfer ( $\tau$ ) for Na. Finally, we find that up-scaling from the  
44 pedon to hillslope scale is possible with geophysical methods for certain pedon  
45 properties. Taken together, these findings suggest that the GPR profiles down  
46 hillslopes can be used to infer lateral thickness variations in pedolith horizons in  
47 different ecologic and climate settings, and to some degree the physical and  
48 chemical variations with depth.

49

50 Keywords: regolith, pedolith, hillslope, climate, vegetation, geophysics,

51

Deleted: In this study, we

Deleted: soil

Deleted: geochemical

Deleted: soil

Deleted: soil

Deleted: soil

Deleted: soil

Deleted: available

Deleted: along

Deleted: soil

Deleted: soil, saprolite

63 **1 Introduction**

64 Weathering of bedrock by biotic and abiotic processes produces regolith which  
65 provides resources for life. Most biota is found in the mobile pedolith, which overlies  
66 the immobile saprolith. The pedolith is replenished with nutrients from the saprolith  
67 through chemical weathering and erosion that drives nutrient uplift towards the  
68 surface (e.g., Porder et al., 2007). The thickness and production of pedolith is  
69 influenced by aspect, topography, composition (mineral content), biota, climate,  
70 tectonically driven rock uplift, and time (e.g., Hilgard, 1914; Jenny, 1994). However,  
71 subsurface variations in pedolith thickness at the scale of hillslopes are difficult to  
72 quantify because of lack of exposure. Thus, subsurface imaging by geophysical  
73 techniques, when calibrated to regolith excavations (pedons), offers a potential  
74 means to characterize spatial variability in pedolith thickness and regolith properties  
75 (e.g., Mellett, 1995; Doolittle and Collins, 1995; Miller et al., 2002). Here, we  
76 evaluate the utility of applying Ground Penetrating Radar (GPR) to map variations  
77 in physical and chemical regolith properties caused by diverse climate and  
78 ecological settings.

79 Previous work has attributed spatial variations in pedolith thickness to hillslope  
80 curvature (Heimsath et al., 1997; Heimsath et al., 1999), which determines the  
81 downslope rate of mass transport assuming a diffusion-based geomorphic transport  
82 law (e.g., Roering et al., 2001). However, this single point information is spatially  
83 restricted and pedon excavations are time-intensive. To further understand spatial  
84 variations in pedolith and saprolith thickness, other approaches such as modeling  
85 (e.g., Scarpone et al., 2016) and geophysical imaging (e.g., see summary in  
86 Parsekian et al., 2015) have been applied. For example, pedolith thickness  
87 variations were extrapolated from Digital Elevation Models (DEMs) in combination  
88 with several different observations at single locations (e.g., Scarpone et al., 2016).  
89 Different geophysical techniques have provided a non- or minimally invasive  
90 approach to view pedolith variations down to the saprolith and bedrock interface  
91 (e.g., Parsekian et al., 2015). Whereas high frequency GPR has proven suitable for  
92 investigating pedolith layering and thickness (e.g., Doolittle et al., 2007; Gerber et

**Formatted:** Normal, Justified, Indent: Left: -0.01 cm, First line: 0 cm

**Deleted:** an upper

**Deleted:** layer (soil),

**Deleted:** is underlain by an

**Deleted:** layer of weathered material (saprolite) that replenishes the soil

**Deleted:** soil

**Deleted:** climate, biota, composition (mineral content),

**Deleted:** sub-surface

**Deleted:** soil

**Deleted:** soil pit

**Deleted:** one

**Deleted:** mean

**Deleted:** soil

**Deleted:** soil

**Deleted:** 2004

**Deleted:** soil

**Deleted:** in

**Deleted:** with stark differences in physical and chemical soil properties

**Deleted:** soil

**Deleted:**

**Deleted:** soil

**Deleted:** saprolite

**Deleted:** soil

**Deleted:** soil

**Deleted:** saprolite

**Deleted:** soil

120 al., 2010; Roering et al., 2010; Dal Bo et al., 2019), other methods such as seismics  
121 (e.g., Holbrook et al., 2014), Electrical Resistivity Tomography (ERT, e.g., Braun et  
122 al., 2009), and low frequency GPR (e.g., Aranha et al., 2002) are better suited to  
123 image [saprolith](#) and bedrock interfaces (e.g., Parsekian et al., 2015). GPR methods  
124 were [also](#) previously used to indirectly measure water flow (e.g., Zhang et al., 2014;  
125 Guo et al., 2020) as well as root density (e.g., Hruska et al., 1999; Guo et al., 2013).  
126 Interpreting the interplay of GPR signals with physical and chemical [regolith](#)  
127 properties is challenging (e.g., Saarenketo, 1999; Sucre et al., 2011; Tosti et al.,  
128 2013; Sarkar et al., 2019).

129 The Chilean Coastal Cordillera (Fig. 1) contains an extreme climate and  
130 vegetation gradient and is a natural laboratory to study the influence of climate and  
131 vegetation on the surface of the Earth in a setting with similar tectonic history and  
132 lithology. The region is home to four study areas of the German-Chilean EarthShape  
133 priority program (www.earthshape.net), where investigations of biotic interactions  
134 with [regolith were](#) conducted (e.g., Bernhard et al., 2018; Oeser et al., 2018). The  
135 study areas were selected to [show a range from](#) arid climate in the northernmost  
136 location ( $\sim 26.1^\circ$  S), to temperate rain forest conditions in the southernmost location  
137 ( $\sim 37.8^\circ$  S). These four study areas [were](#) investigated to qualitatively and  
138 quantitatively describe the differences between the four settings. Our previous work  
139 in these areas has identified [from field observations and GPR based methods an](#)  
140 [increase](#) in [pedolith](#) thickness from north to south and major and trace element  
141 compositional variations within pedons (e.g., Bernhard et al., 2018; Oeser et al.,  
142 2018; Dal Bo et al., 2019). However, [in our previous GPR work \(Dal Bo et al., 2019\)](#)  
143 [we were not able to present](#) a detailed comparison of [physical, chemical,](#) and  
144 [regolith](#) observations [which has](#) yet to be [reported for](#) these areas.

145 [In this paper we build upon the previous work of Dal Bo et al. \(2019\) and compare](#)  
146 [the pedon measured physical and chemical observations \(from Bernhard et al.](#)  
147 [\(2018\) and Oeser et al. \(2018\)\) to a large newly acquired GPR data set from the](#)  
148 [same area to gain insight into regolith variations along a climate and ecological](#)  
149 [gradient. Our approach is to relate GPR observations adjacent to pedons to depth](#)

Deleted: saprolite

Deleted: also

Deleted: the distribution of

Deleted: soil

Deleted: within the sub-surface

Deleted: and not well-understood

Deleted: 1999

Deleted: it

Deleted: sub-

Deleted: a

Deleted: critical zone processes are

Deleted: due

Deleted: the

Deleted: (

Deleted: and

Deleted: (38

Deleted: are

Deleted: both

Deleted: so far

Deleted: increases

Deleted: soil

Deleted: geophysical, geochemical

Deleted: soil

Deleted: is

Deleted: conducted in

Deleted: In this study, we investigate how physical as well as chemical observations measured at point locations (pedons) relate to GPR observations to gain further insight into the sub-surface variations. In general, we find that GPR signals can be correlated to changes in soil

180 [varying regolith properties](#) caused by weathering as well as to evaluate if these  
181 [properties can be extrapolated along a hillslope using GPR transects](#). In doing this,  
182 [we test the hypothesis that if weathering processes produce depth varying physical](#)  
183 [and chemical changes in regolith observed in pedons](#), then (a) GPR based  
184 [observations of these locations should produce observable changes in the GPR](#)  
185 [envelope and reflectors correlative to weathering horizons](#), and (b) GPR can be  
186 [used to up-scale geochemical observations from pedons to the hillslope scale](#). In  
187 [general, we find that our new GPR measurements can be correlated to changes in](#)  
188 [pedolith](#) physical properties if these changes are of sufficient magnitude and laterally  
189 coherent. If such a correlation is observed, we discuss the links between the  
190 physical and chemical properties. The comparison of physical and chemical  
191 properties with field observations and GPR data helps to better understand the  
192 [regolith](#) at point locations (e.g., [pedolith](#) thickness) and in some cases allows for up-  
193 scaling point observations to the hillslope scale along a GPR measurement profile.  
194

Deleted: sub-surface

Deleted: soil

## 195 2 Study areas

196 [From north to south \(Figs 1 and 2\), the four selected](#) study areas in the climatic  
197 and vegetation gradient observed in the Chilean Coastal Cordillera are: a) Pan de  
198 Azúcar (~26.1° S); b) Santa Gracia (~29.8° S); c) La Campana (~33.0° S); and d)  
199 Nahuelbuta (~37.8° S). [The study areas were investigated for regolith physical and](#)  
200 [chemical properties by Bernhard et al. \(2018\) and Oeser et al. \(2018\) as well as](#)  
201 [studied with GPR by Dal Bo et al. \(2019\) \(see Tables 1 and 2\)](#).

Deleted: Four primary

Deleted: are investigated

Deleted: (Fig. 1 and 2; Table 2). From N to S, the four selected areas...

### 202 2.1 General climate, vegetation, and geologic setting

204 The Chilean Coastal Cordillera with its climate and vegetation gradient is a  
205 natural laboratory to study the influence of climate and vegetation on denudation  
206 (Fig. 1). From [north to south](#) (~26° to 38° S), present climate ranges from arid to  
207 humid-temperate. The mean annual precipitation increases from [nearly](#) zero to  
208 ~1500 mm yr<sup>-1</sup>, and mean annual temperature decreases from ~20° C to ~5° C.

Deleted: N

Deleted: S

Deleted: close to

218 [Vegetation cover increases from nearly zero to ~100%](#). The flora consists of small  
219 shrubs, geophytes and annual plants (Armesto et al., 1993) in the [north](#) and  
220 changes to lower-stature deciduous trees and shrubs intermix with tall evergreen  
221 mixed forest in the [south](#).

Deleted: N

Deleted: S. Vegetation cover increases from close to zero to ~100%....

222 Climate and vegetation in the primary study areas changed over time from the  
223 Last Glacial Maximum (LGM) to present. Mean annual precipitation during the LGM  
224 was higher than at present in all four study areas (Mutz et al., 2018). Mean annual  
225 temperature during the LGM was lower than at present except in the southernmost  
226 study area where mean annual temperature stayed the same (Mutz et al., 2018).  
227 Hence, the climate gradient observed today is comparable to the gradient during the  
228 LGM. Even though the climate was wetter and cooler during the LGM, no glaciers  
229 covered any of the study areas (Rabassa and Clapperton, 1990). [Because of](#) these  
230 climatic changes over time, vegetation zones during the LGM were shifted  
231 northward by ~5° and vegetation cover was slightly (~5-10%) lower compared to  
232 present (Werner et al., 2018). This shift of vegetation zones to the [north](#) and the  
233 decrease in vegetation cover also likely influenced the fauna present, but to an  
234 unknown degree.

Deleted: Due to

Deleted: N

235 To compare the effect of climate and vegetation on [pedolith](#) thickness and GPR  
236 observations, differences in lithologies need to be minimal. However, these  
237 conditions are not always fulfilled and need to be taken in to account. Whereas  
238 bedrocks in Pan de Azúcar, La Campana, and Nahuelbuta are granites to  
239 granodiorites, the bedrocks in Santa Gracia range from Granodiorites to Gabbros  
240 (Oeser et al., 2018). Hence, the parent material in Santa Gracia is lower in  $\text{SiO}_2$ -  
241 content (50-65%) in comparison to the other three study areas ( $\text{SiO}_2$ -content >65%).  
242 Chemical weathering and physical erosion, which in turn [influence pedolith](#)  
243 formation and thickness, [may be affected by this difference](#).

Deleted: soil

Deleted: the

Deleted: may be affected by this difference

Deleted: influences soil

## 245 2.2 [Regolith](#) Characteristics

Deleted: Soil

246 In each study area, [regolith transects \(Figs 2 and 3; Table 1\)](#) from a catena  
247 consisting of three [pedons](#) on the S-facing slope (top-slope, mid-slope, and toe-

Deleted: depth profiles

Deleted: profiles

260 slope) and one [pedon](#) on the N-facing slope (mid-slope) were described, sampled,  
 261 and analyzed (see [Bernhard et al., 2018](#); [Oeser et al., 2018](#); [Schaller et al., 2018](#);  
 262 [Dal Bo et al., 2019](#)). [Only one pedon was investigated in the N-facing slopes due to](#)  
 263 [time and financial restrictions. In addition, transect lengths in some settings are](#)  
 264 [limited due to the availability of weathered hillslopes in the same lithologies \(e.g.,](#)  
 265 [Pan de Azúcar; Fig. 3A\) as well as restriction of access due to intense vegetation](#)  
 266 [\(e.g., Nahuelbuta; Fig. 3D\).](#)

267 [These previous](#) studies from pedons in each area identify O, A, B, and C horizons  
 268 [that overlie weathered bedrock \(for complete characterization and interpretation of](#)  
 269 [the pedons see Fig. 2 in Bernhard et al. \(2018\) and Figs 3 to 6 in Oeser et al. \(2018\)\).](#)

270 In this study, we refer to depth profiles as regolith profiles that are composed of a  
 271 mobile [pedolith](#) that includes the A and B horizons, and an immobile [saprolith](#)  
 272 [including](#) the C horizon.

273 In Pan de [Azúcar](#), the [regolith](#), a regosol ([IUSS Working Group WRB, 2015](#)),  
 274 consists of [A and B horizons with a combined thickness of 20 to 25 cm and an](#)  
 275 [underlying saprolith \(the C horizon\), which is coarse-grained and jointed \(Oeser et](#)  
 276 [al., 2018\).](#) The total organic carbon content [of the A and B horizons](#) is <0.1%  
 277 ([Bernhard et al., 2018](#)). [Angular](#) fragments in the [pedolith](#) increase in size (> 1 mm)  
 278 with depth. The average bulk density of the [A and B horizons](#) is 1.3 g cm<sup>-3</sup>. In Santa  
 279 Gracia, [the 30 to 55 cm thick pedolith overlying the saprolith is a cambisol \(IUSS](#)  
 280 [Working Group WRB, 2015\).](#) Total organic carbon content [of the A and B horizons](#)  
 281 is 0.4%. Whereas the A horizon consists of a silt- to fine sand-sized matrix  
 282 supporting up to 2 mm sized fragments, the underlying B horizon shows a  
 283 transitional increase of fragments to a coarse fragment-supported fine-grained  
 284 matrix. [The weathered granodiorite of the saprolith consists of up to 1 cm-sized](#)  
 285 [fragments which are surrounded by fine-grained material and fine roots](#) ([Oeser et](#)  
 286 [al., 2018](#)). The average bulk density [of the pedolith](#) is 1.5 g cm<sup>-3</sup>. The [regolith](#) in La  
 287 Campana [is a cambisol \(IUSS Working Group WRB, 2015\).](#) The A and B horizons  
 288 are 35 to 60 cm thick and have a total organic carbon content of 1.9% ([Bernhard et](#)  
 289 [al., 2018](#)). The fine sand- to silt-sized A horizon contains fragments of up to 3 mm.

**Deleted:** profile

**Deleted:** Fig. 3;

**Deleted:** also

**Deleted:** Previous soil

**Deleted:** (e.g., Bernhard et al., 2018)

**Deleted:** e.g.,

**Deleted:** .,

**Deleted:** ).

**Deleted:** follow the approach of Riebe and Granger (2013) and ...

**Deleted:** soil layer

**Deleted:** saprolite layer represented by

**Deleted:**

**Deleted:** Azúcar

**Deleted:** soil is part of

**Deleted:** and

**Deleted:** thick A and B

**Deleted:** .

**Deleted:** la

**Deleted:** The observed angular

**Deleted:** soil

**Deleted:** The underlying saprolite is coarse-grained and jointed (Oeser et al., 2018).

**Deleted:** soil layer

**Deleted:** The cambisol in

**Deleted:** consists of

**Deleted:** layers of soil with A and B horizons

**Deleted:** saprolite (Bernhard et al., 2018). The total

**Deleted:** soils and saprolites

**Deleted:** form

**Deleted:** . The soil layers consisting of

**Deleted:** la

322 The matrix in the underlying B horizon is coarsening downwards and the number of  
 323 fragments increases such that the horizon shifts from matrix- to clast-supported. [In](#)  
 324 [the saprolith, which shows a granodioritic fabric, fine roots are common and](#)  
 325 [fractures are abundant \(Oeser et al., 2018\).](#) The average bulk density is 1.3 g cm<sup>-3</sup>.  
 326 The [regolith](#) in Nahuelbuta, [an umbrisol \(IUSS Working Group WRB, 2015\)](#), consists  
 327 of a 60 to 90 cm thick [pedolith](#) and a readily disaggregating [saprolith](#). Total organic  
 328 carbon content in these [pedoliths](#) is 6.1% (Bernhard et al., 2018). The A horizon is  
 329 composed of silt-sized particles forming nodular [aggregates](#). In the upper part there  
 330 are up to 1 mm large quartz grains embedded whereas the lower part contains large  
 331 fragments. The fine sand-sized matrix of the transitional B horizon hosts subangular  
 332 fragments. The amount and size of these fragments increases with depth. The  
 333 average bulk density of the [pedolith](#) is 0.8 g cm<sup>-3</sup>.

Moved (insertion) [1]

Deleted: umbrisol

Deleted: soil layer (A and B horizons)

Deleted: saprolite. The total

Deleted: soils

Deleted: la

Deleted: soil

Deleted: soil layer

### 335 **3 Data compilation and methods**

336 New data from [25](#) GPR profiles in the four study areas were collected at  
 337 frequencies of 500 and 1000 MHz. These data are compared to physical and  
 338 chemical properties from point locations (pedons) from previous studies (Bernhard  
 339 et al., 2018; Oeser et al., 2018). [Unfortunately, no regolith water content was](#)  
 340 [measured in samples from the pedons excavated in 2016. The](#) new GPR profiles  
 341 [\(collected in 2017\)](#) complement previous GPR data collected [2016](#) at the same  
 342 frequencies, in the same catchments (Dal Bo et al., 2019). The difference between  
 343 this study and that of Dal Bo et al. (2019) lies in the new, more extensive, GPR data  
 344 coverage, [the analysis of regolith water content in augers in the study areas,](#) and [its](#)  
 345 comparison to physical and chemical subsurface variations.

Deleted: 32

Deleted: These

Deleted: the

Deleted: of it

Deleted: and physical

Deleted: treatment on

Deleted: layers

Deleted: need fixed

Deleted: translating

Deleted: to

Deleted: relevant for

Deleted: need

346 Using [physical and](#) chemical properties collected in pedons to understand the  
 347 corresponding radar signatures is a difficult task requiring multiple [steps](#). First, it  
 348 would [require identifying](#) relationships [between](#) the measured pedon properties [and](#)  
 349 corresponding permittivity changes [in](#) the radar signal. Second, it would [require](#) a  
 350 radar forward model that successfully predicts the convolution of the emitted radar

370 pulse with the [subsurface](#) reflectivity. This includes handling constructive and  
 371 destructive interference caused by closely-spaced [vertical](#) permittivity changes. For  
 372 applications [to regolith](#) this is currently not possible because the permittivity  
 373 relationships are unclear. We therefore take a step back from the more  
 374 sophisticated methods, and use simpler statistical metrics [to isolate regolith](#)  
 375 properties (i.e. Pearson correlation) or combinations thereof (i.e. Principal  
 376 Component Analysis) that may explain parts of the radar signatures.

- Deleted: sub-surface
- Deleted: among others
- Deleted: in the vertical.
- Deleted: on soil,
- Deleted: already
- Deleted: trying
- Deleted: some

### 378 3.1 Data compilation

379 In this study, GPR data are compared to previously published [pedolith](#) and  
 380 [saprolith](#) physical and chemical properties (Table 2) such as: 1) bulk density, grain  
 381 size distribution, [acid and base properties](#) - pH, and cation exchange capacity - CEC  
 382 (Bernhard et al., 2018); and 2) Loss On Ignition - LOI, Chemical index of Alteration  
 383 - CIA, mass transfer coefficient -  $\tau$ , and volumetric strain -  $\epsilon_{\text{strain}}$  (Oeser et al., 2018).

- Deleted: soil
- Deleted: saprolite
- Deleted: 1
- Deleted: soil

384 The grain size distributions provide a measure of the weight percent of different  
 385 grain sizes smaller than 2 mm in the regolith, and the bulk density provides a  
 386 measure of how dense the [pedolith](#) and [saprolith](#) material is packed. The  
 387 geochemical data used provide major and trace element analysis, [pH](#), and [CEC](#).  
 388 Major and trace element [analyses](#) allow the investigation of the [LOI](#), [Tau  \$\tau\$](#) , and  
 389 volumetric strain  $\epsilon_{\text{strain}}$ . The degree of weathering can be quantified by [CIA](#) which is  
 390 sensitive to the removal of alkalis such as calcium, sodium, and potassium from  
 391 feldspars (Nesbitt and Young, 1982).  $\tau$  reflects chemical gains and losses  
 392 during weathering based on the elemental concentrations of mobile and immobile  
 393 elements in weathered and unweathered material (e.g., Brimhall et al., 1985;  
 394 Chadwick et al., 1990),  $\epsilon_{\text{strain}}$  in a regolith is based on the density  $\rho$  ( $\text{g cm}^{-3}$ ) and  
 395 immobile element concentrations of the weathered regolith in comparison to the  
 396 unweathered bedrock indicating volumetric gain or loss (Brimhall and Dietrich,  
 397 1987).

- Deleted: ,
- Deleted: regolith
- Deleted: soil
- Deleted: saprolite
- Deleted: the acid
- Deleted: base properties (pH) and cation exchange capacity (
- Deleted: )
- Deleted: analysis
- Deleted: loss on ignition (
- Deleted: ), the chemical index of the mass transfer coefficient ( $\tau$ ), and the
- Deleted: ( $\epsilon$
- Deleted: ). LOI is a measure of the loss of volatile substances in a material due to excess heating (1000°C), thereby reflecting the amount of soil organic matter.
- Deleted: the
- Deleted: The mass transfer coefficient ( $\tau$
- Deleted: )

427 [GPR signals are sensitive to regolith water content variations with depth \(e.g.,](#)  
 428 [Steelman et al., 2012; Ardekani et al., 2014\)](#). In addition to our compilation of  
 429 [previously published chemical and physical properties, we present here newly](#)  
 430 [collected regolith water content data from regolith augers in Santa Gracia, La](#)  
 431 [Campana, and Nahuelbuta \(supplement Tables S3A to C\)](#). Although this data  
 432 [provides insight into regolith water content variations with depth, regularly spaced](#)  
 433 [sampling with depth was not possible in the field. As a result, the regolith water](#)  
 434 [content data are sparse, and not directly overlying the GPR profile locations. Given](#)  
 435 [the sparseness of this data, we were not able to include it in our correlations or](#)  
 436 [correlation and PCA analysis \(described below\), but we do discuss trends present](#)  
 437 [in the regolith water content \(gravimetric basis\) with depth and potential implications](#)  
 438 [for the rest of our analysis. Furthermore, we note that the GPR data were not](#)  
 439 [collected with an approach that allowed for the inversion for regolith water content](#)  
 440 [\(e.g., Steelman et al., 2012\)](#).

### 442 3.2 Ground Penetrating Radar (GPR)

443 Ground Penetrating Radar (GPR), a geophysical technique based on the  
 444 emission of pulsed electromagnetic waves into the subsurface, [are applied in this](#)  
 445 [study for](#) frequencies of 500 and 1000 MHz [\(for more details see Dal Bo et al., 2019\)](#).  
 446 [Fourteen new](#) transects going from hillslope toe (near valley) to top (ridge crest) [are](#)  
 447 collected [crossing the pedons](#) where physical and chemical properties were  
 448 collected (Figs. 2 and 3). Of these [14 transects](#), two were collected in the Pan de  
 449 Azúcar study area [\(for 500 and 1000 MHz\)](#), six in Santa Gracia [\(for 500 and 1000](#)  
 450 [MHz\)](#), three in La Campana [\(for 500 and 1000 MHz\)](#), and three in Nahuelbuta [\(only](#)  
 451 [for 500 MHz\)](#). Wide-angle-reflection-refraction (WARR) are used to retrieve velocity  
 452 and physical properties at the point scale. For each pedon, a WARR is measured in  
 453 [a relatively flat location](#) (red stars, Fig. 2).

454 [GPR data were processed and analyzed using MATLAB as described in Dal Bo](#)  
 455 [et al. \(2019\)](#). In addition, [signal](#) envelopes were calculated using a Hilbert transform  
 456 (Green, 2004; Liu and Marfurt, 2007). At each pedon location, a certain number of

**Deleted:** ) is

**Deleted:** and here

**Deleted:** are applied. The electromagnetic waves are reflected and scattered in the presence of dielectric contrasts at depth. The back-propagated reflected wave is then received at travel times, which depend on the depth-variable electromagnetic wave velocity  $v$ . The velocity of the media is dictated by the relative dielectric permittivity  $\epsilon_r$  (Jol, 2009). The attenuation of the waves can be linked to the electrical conductivity  $\sigma$ . The vertical resolution depends on the system's bandwidth and the wave velocity and is in our case approximately 0.07 m for 500 MHz and 0.03 m

**Deleted:** 1000 MHz. Surface GPR can be measured in two ways including: 1) Common-Offset Profiling (COP) and 2) Common-midpoint (CMP) or wide-angle-reflection-refractions (WARR) measurements (

**Deleted:** also

**Deleted:** COPs measure traveltimes versus spatial position along specific transects with two antennae at fixed offsets. Here, this was done along profiles crossing the pedons (e.g., Fig. 2 and 3). WARRs are used to retrieve velocity and physical properties at the point scale with variable antennae spacing. Specifically, for each pedon a WARR was measured in a relatively flat location by keeping the transmitter position fixed at the pedon location and by moving the receiver towards the transmitter with a step size varying between 0.01 and 0.05 m depending on the deployed frequency. In such way, the move-outs of linear events (air wave and ground wave) and of hyperbolic events (sub-surface reflections) could be identified using the underlying assumption that internal reflectors are not dipping. Twenty-eight COP

**Deleted:** were

**Deleted:** in the four study areas using 500 and 1000 MHz GPR antennae (Sensor and Software Inc.). The average trace spacing of these vary between 0.01 and 0.05 m depending on frequency and location. These transects were chosen in such way as to run between pedons,

**Deleted:** the previously described

**Deleted:** Bernhard et al., 2018; Oeser et al., 2018).

**Deleted:** 28 profiles

**Deleted:** ,

**Deleted:** ,

**Deleted:** ,

**Deleted:** . Each profile was measured twice to total 28 (at the two frequencies). The pedon locations formed the basis for comparison to the GPR data as ground-truth data and WARRs and COPs were collected specifically at these positions

**Deleted:** 2). Additionally, four perpendicular GPR crosslines (perpendicular to the transects) were measured at both the 500 and 1000 MHz in the La Campana and Nahuelbuta study ... [1]

**Deleted:** GPR data were processed and analyzed similar to Dal Bo et al. (2019) using MATLAB. The GPR data processing

**Moved down [2]:** (e.g., Jol, 2009).

**Deleted:** The direct air wave between receiver and transmitter was muted. Similar to Dal Bo et al. (2019), the newly measured

535 traces depending on the measurement step size (i.e. between 10 and 50) were  
536 sampled for 0.5 m uphill and 0.5 m downhill the pedon and laterally averaged for  
537 comparison to the pedon physical and chemical properties. The averaging assumes  
538 that both chemical and GPR signatures do not change with depth across that  
539 interval, an assumption that may not hold everywhere. As the GPR envelope is  
540 directly related to the electric impedance (Telford et al., 1990; Jol, 2009), the  
541 envelope onset and energy intervals could be compared to variations in physical,  
542 and potentially chemical, [regolith](#) properties.

**Deleted:** soil

### 544 3.3 Statistical Correlation and Principal Component Analysis

545 Comparison between the [physical and](#) chemical pedon information (Bernhard et  
546 al., 2018; Oeser et al., 2018) and GPR data was conducted. [Where available](#), we  
547 used the bulk density, clay content, LOI, CIA, Tau ( $\tau$ ), volumetric strain ( $\epsilon_{\text{strain}}$ ), pH,  
548 and CEC for comparison to the GPR 500 and 1000 MHz antennae envelope data.  
549 The GPR envelopes were resampled and averaged, such that the depth intervals  
550 were the same as for the derivatives of the [regolith](#) data (see Table S2). Furthermore,  
551 because the envelope of GPR data is sensitive to changes along the vertical  
552 direction, we also calculated the vertical gradient of the ground truth information at  
553 each sampled depth using a centered difference approximation. Following this, the  
554 R package function corrplot (Wei, 2012) was used to calculate the Pearson's  
555 correlation coefficient to identify correlations between the variables (Sedgwick,  
556 2012). [We further](#) conducted a multivariate analysis of the data [based on](#) principal  
557 component analysis (PCA; Wold et al., 1987). This was done using the factoextra R  
558 package (Kassambara, 2017). [Correlation coefficients and PCA are done for each](#)  
559 [study area along the entire climate gradient](#).

**Deleted:** and physical

**Deleted:** two different ways. First, we carried out a correlation analysis using the Pearson' correlation coefficient ( $r$ ). More specifically

**Deleted:** soil

**Deleted:** This analysis was done considering the entire climate and vegetation gradient and within each location. Both the original data and the derivatives were used to explore which of the two approaches delivered meaningful insights.¶  
Second, we

**Deleted:** using a

**Deleted:** for both the entire climate gradient and within each study area

**Deleted:** After each PCA analysis, a scree plot was evaluated to investigate how much variance was included in each principal component (PC, Bro and Smilde, 2014). In this study, at least 70% of the variance was among the first two PCs, which were then further analyzed. The contribution of each variable to the first and second PC was computed using the eigenvalues and eigenvectors from the covariance matrix (Abdi and Williams, 2010). This resulted in a plot where the x-axis is PC1 and the y-axis is PC2 and each variable is displayed as a vector with a specific direction and length that indicate the magnitude and direction of the contribution to each PC

**Deleted:** from

## 561 4 Results

562 Physical and chemical properties [of](#) pedons are shown with the 500 and 1000  
563 MHz GPR profiles and their envelopes with depth as well as investigated

590 correlations and [PCA results](#) for the four study areas ([Figs 4 to 11](#); [Figs S1 to S12](#);  
591 [Table 3](#); Tables S1A to D, S2A to D, [S3A to C](#), and S4A to E). For brevity,  
592 [comparisons between pedon observations and GPR data](#) are presented [only](#) for the  
593 S-facing mid-slope positions in the main text ([Figs 4, 6, 8, and 10](#)) and the remaining  
594 locations are provided in the supplementary material. Note that the envelopes are  
595 averaged over the [common offset profile](#) data, collected over a lateral distance of 1  
596 m in total, and are therefore not point information. Given that the [pedolith](#) thickness  
597 increases towards the southern study areas, the 1000 MHz GPR [antenna](#) is  
598 interpreted for the northern two [study areas](#) Pan de Azúcar and Santa Gracia,  
599 whereas in La Campana and Nahuelbuta the 500 MHz GPR signal was used  
600 because it has a deeper penetration depth. However, we show results below for  
601 both frequency antennas to demonstrate the difference in penetration depth and  
602 resolution between the two antennae. Details for each study area (from [north](#) to  
603 [south](#)) follow.

- Deleted: PCAs
- Deleted: Fig.
- Deleted: and supplement
- Deleted: and supplement
- Deleted: S3
- Deleted: only the
- Deleted: Fig.
- Deleted: COP
- Deleted: soil
- Deleted: antennae
- Deleted: (
- Deleted: )
- Deleted: study areas

- Deleted: N
- Deleted: S

#### 605 4.1 Pan de Azúcar (northern most [and driest](#) study area)

606 In Pan de Azúcar ([Figs 1, and 2A](#)), a gradual transition from the B to the C horizon  
607 was visually observed in the pedons at 20 to 40 cm ([shaded gray areas after](#)  
608 [Bernhard et al. \(2018\); Fig. 4; Figs S1 to S3](#)), whereas the mobile [and](#) immobile  
609 boundary is considered to be at 20 to 25 cm [\(black lines after Oeser et al., \(2018\);](#)  
610 [Fig. 4; Figs S1 to S3\)](#). [No water content measurements for this area were available](#)  
611 [due to poor recovery of auger samples from the impenetrable substrate](#). The  
612 available physical properties for this location do not indicate a strong change in  
613 material properties with depth. LOI and CIA indicate a minor change in properties at  
614 ~20 cm depth. A maximum in the energy envelope in the 1000 MHz frequency is  
615 present at about 20 to 30 cm [and](#) could be related to the transition of material  
616 properties between the B and C horizons and the location of mobile [and](#) immobile  
617 boundary observed in the field.

- Deleted: Fig.
- Deleted: ,
- Deleted: /
- Deleted: (shaded gray areas and
- Deleted: line, Fig. 4,
- Deleted: S1 to S3).

- Deleted: that
- Deleted: /

618 Due to the sparse depth information for bulk density and clay content, the  
619 statistical analyses for this location [were](#) not very insightful. Whereas clay content

- Deleted: was

644 shows a medium correlation (0.54) with the 1000 MHz GPR envelope, no strong  
645 correlation between LOI, CIA, [Tau](#)  $\tau$ , and the 1000 MHz GPR envelope could be  
646 found (Table [3](#)). In the PCA, three [principal](#) components (PC) explain over 80% of  
647 the variance (Table S4A). PC1 has the [biggest](#) contribution from CIA, clay content,  
648 and the 500 MHz envelope whereas PC2 has the [biggest](#) contribution from LOI, the  
649 1000MHz envelope, and  $\tau$  of Na and Zr (Fig. 5).

Deleted: S3  
Deleted: primary  
Deleted: bigger  
Deleted: bigger

#### 650 651 4.2 Santa Gracia

652 In Santa Gracia ([Figs 1 and 2B](#)), a gradual transition from the B to the C horizon  
653 was observed in the field between 20 to 60 cm depth (shaded gray region Fig. 6;  
654 [Figs S4 to S6](#)). The boundaries between the [pedolith and saprolith](#) were observed  
655 between 30 to 55 cm depth. [Water content near pedon locations ranges between](#)  
656 [7.6% to 1.8% and is highly variable with sample locations and with no clear spatial](#)  
657 [or depth dependent trend \(Table S3A\)](#). Bulk density and volumetric strain show  
658 slight changes around 15 and 30 cm depth. Whereas LOI and CIA do not show any  
659 changes with depth,  $\tau$  shows changes between 30 and 50 cm depth. The 500 and  
660 1000 MHz GPR profiles and envelopes show increased irregular and strong  
661 reflections at ~25 cm (1000 MHz) and 45 cm (500 MHz) depth, and also maximums  
662 in the envelope at ~25 cm (1000 MHz) and 45 cm (500 MHz) depths. These  
663 variations in the reflections and maximums in the envelopes coincide with either the  
664 top or central position of the transition from the B to the C horizon.

Deleted: Fig.  
Deleted: ,  
Deleted: , Fig.  
Deleted: mobile/immobile layers in the pedon

665 A weak to moderate correlation (~0.[30](#)) between clay content as well as CIA and  
666 the 1000 MHz GPR envelope is present (Table [3](#)). Results from a PCA analysis of  
667 the Santa Gracia data indicate that 3 components explain over 80% of the observed  
668 variance (Table S4B). PC1 explains over 35% of the variance, and includes bulk  
669 density, CIA, and the 500 and 1000 MHz envelopes (Fig. 7). PC2, explaining 31%  
670 of the variance, includes clay content, LOI, and  $\tau$  of Na and Zr.

Deleted: 3  
Deleted: S3

#### 671 672 4.3 La Campana

683 Field observations from the La Campana area (Figs 1 and 2C) document a layer  
684 of cobbles (5 to 10 cm diameter) between the A and B horizon at a depth of ~30 cm  
685 (Bernhard et al., 2018). The transition between the B to C horizons does not contain  
686 rock fragments. The transition from the B to C horizon (shaded gray area, Fig. 8)  
687 and the mobile and immobile boundary (black line, Fig. 8) are observed at 34 to 110  
688 cm and 35 to 60 cm, respectively (see also Figs S7 to S9). The pedolith extends  
689 deeper in La Campana than in Pan de Azúcar or Santa Gracia and physical  
690 properties were available for greater depths. Bulk density and grain size change  
691 gradually with depth and no pedolith thickness could be determined. Also, LOI, CIA,  
692 and  $\tau$  do not show an abrupt change in regolith properties. [Water content near  
693 pedons ranges between 3.1% to 1.5% and shows only a slight \(~0.5%\) decrease  
694 between depths of ~30 to 90 cm \(Table S3A\).](#) Reflection hyperbolas and irregular  
695 reflection horizons appear in the 500 and 1000 MHz GPR data at about 40 to 60 cm  
696 depth above the B to C horizon transition. The second peaks of the 500 and 1000  
697 MHz GPR envelopes coincide with the B to C horizon transition.

698 In contrast to the previous study areas, the 500 MHz GPR envelope correlates  
699 moderately with CIA (0.56), pH (-0.57), and CEC (-0.39, Table 3). Three  
700 components from the PCA analysis explain about 80% of the total variance (Table  
701 S4C). PC1 (~35% of the total variance) includes LOI,  $\tau$ , and CEC, whereas PC2  
702 (31%) contains CIA, volumetric strain  $\epsilon_{\text{strain}}$ , and the envelopes (Fig. 9). PC3 is  
703 dominated by pH as well as  $\tau$  of Zr. In general, whereas the first energy interval  
704 (1000 MHz) could be attributed to the stone layer between the A and B horizon, the  
705 second energy interval occurs close to (<10 cm) with the mobile and immobile  
706 boundary (Fig. 8).

#### 707 708 4.4 Nahuelbuta (southernmost and wettest study area)

709 In Nahuelbuta, the B horizon contains pebbles and cobbles at around 60 to 80  
710 cm depth (Bernhard et al., 2018). The B to C horizon transition appears at 50 to 100  
711 cm depth (shaded gray region, Fig. 10; see also Figs S10 to S12). The mobile and

Deleted: Fig.

Deleted: ,

Deleted: /

Deleted: Fig.

Deleted: mobile soil layer

Deleted: soil

Deleted: S3

Formatted: Subscript

Deleted: /

Deleted: Fig.

Deleted: /

722 immobile boundary was identified at 60 to 90 cm depth (Oeser et al., 2018). Density  
723 measurements in the pedon indicate a transition in bulk density between about 30  
724 to 60 cm depth where the grain size distribution also changes. The LOI and  $\tau$   
725 generally show large changes with depth, in contrast to the CIA and volumetric strain  
726 which are more homogenous with depth. In general water content near pedons and  
727 in near-surface (10 to 30 cm depth) samples is between 23 and 39% and decreases  
728 ~3% to ~10% over regolith depths of 30 to 90 cm (Table S3A). In addition, water  
729 content increases from top- to toe-position in the S-facing slope and is lower in the  
730 N-facing mid-slope position than in the S-facing position. The 500 MHz GPR profile  
731 indicate the existence of point targets/objects appearing as reflection hyperbola or  
732 undulating features at depths greater than 60 cm. This depth is approximately the  
733 same depth at which the mobile and immobile boundary was identified, as well as  
734 changes in the physical properties (e.g. bulk density, percent sand) and chemical  
735 properties (LOI, Tau  $\tau$ ). The hyperbolas do not add up coherently during the lateral  
736 averaging and therefore do not produce a significant energy interval in the average  
737 envelope. The envelope is dominated by the energy intervals given by two  
738 reflections at about 30 to 50 cm depth. The lower set of these energy intervals could  
739 be linked with the upper physical pedolith boundary.

740 Results from the correlation analysis indicate that the 500 MHz GPR envelope  
741 is strongly positively correlated with bulk density (0.74), strongly inversely correlated  
742 with LOI (-0.60), and moderately inversely or positively correlated with clay content  
743 (-0.37), pH (0.46), and CEC (-0.53) (Table 3). Results from the PCA analysis show  
744 that two PC components explain ~75% of the variance. PC1 (~57 %) includes bulk  
745 density, clay content, LOI, and CEC, and PC2 (~18 %) contains  $\tau$  of Zr and pH (Fig.  
746 11; Table S4D). In general, as the 500 MHz GPR envelope signal correlates well  
747 with bulk density and clay content, the envelope signal reflects changes in regolith  
748 properties.

749

Deleted: .

Deleted: also

Deleted: 60cm

Deleted: /

Deleted:  $\tau$  properties.

Deleted: soil

Deleted: 6

Deleted: S3

Deleted: whereas

Deleted: soil

760 **5 Discussion**

761 Here we evaluate the [physical](#), chemical, and geophysical observations from the  
762 pedons. Using this information, we attempt to up-scale information from the pedons  
763 to the hillslopes scale along the GPR transects.

**Deleted:** physical,

**Deleted:** Potential soil thickness over hillslopes is discussed in light of hillslope, aspect, and the climate and vegetation gradient from N to S...

765 **5.1 Synthesis of GPR data with physical and chemical properties from point**  
766 **locations**

767 GPR data image [subsurface](#) changes that could be caused by [variations](#) in  
768 physical (e.g., bulk density, grain size variation, water content) [and](#) chemical  
769 properties (e.g., pH, CEC, CIA). The interplay between these different properties  
770 can have a complicated influence on the GPR signal and therefore [can be](#) difficult  
771 to disentangle. Disentangling any relationship between GPR data and physical and  
772 chemical properties is further complicated [because](#) not all properties influencing  
773 GPR data are measured [in the pedons](#) (e.g., water content; Jol, 2009). In addition,  
774 the determination of [the boundary](#) between the [pedolith and saprolith](#) in the field  
775 causes its own problems [because](#) observed changes are [not discrete but](#)  
776 transitional over a depth interval of 5 to 10 cm. In the following, we start by  
777 discussing if GPR data can be used to image [pedolith](#) thickness as well as physical  
778 and chemical properties at the pedon locations where *in-situ* observations were  
779 made in each study area.

**Deleted:** in material properties

**Deleted:** changes

**Deleted:** ), or potentially

**Deleted:** as

**Deleted:** soil thickness (i.e.,

**Deleted:** mobile/immobile layers)

**Deleted:** as

**Deleted:** and not discrete.

**Deleted:** soil

**Deleted:** Fig.

**Deleted:** , 5

**Deleted:** Fig.

**Deleted:** shows

**Deleted:** soil

**Deleted:** deep (sub-soil depth) interfaces

**Deleted:** soil

**Formatted:** English (UK)

**Deleted:** Fig.

**Formatted:** English (UK)

**Deleted:** soil

**Deleted:** saprolite layers

**Deleted:** here

**Deleted:** antennae

**Deleted:** favourable

**Deleted:** soil/saprolite

780 In Pan de Azúcar ([Figs 4](#), and [5](#); [Figs S1](#) to [S3](#)), the locations where GPR data  
781 can be compared to pedons [show](#) low variability in the observed [pedolith](#) thickness  
782 (~20 to 30 cm) at each pedon location. Whereas the 500 MHz signal shows [the](#)  
783 [interface with the saprolith](#), the maximum in the 1000 MHz energy interval signal  
784 agrees with the [pedolith](#) thicknesses observed in the field (Fig. 4 and [Figs S1](#) to [S3](#)),  
785 However, the boundary between [the pedolith](#) and [saprolith](#) is probably too shallow  
786 to be detected with the 1000 MHz [antenna](#). An even higher frequency would be  
787 [required](#) to detect the [pedolith and saprolith](#) boundary. Hence the Pearson  
788 correlations and PCA results from Pan de Azúcar are restricted not only because of  
789 GPR analysis but also due to restricted physical properties. The [physical and](#)

817 chemical properties correlate only weakly to moderately with the 1000 MHz  
818 envelopes (Table 3). The PCA results indicate that bulk density is not likely  
819 correlated with either the 1000 MHz signal or LOI. In Pan de Azúcar, LOI does not  
820 represent organic matter because regoliths of arid zones generally have low or no  
821 organic matter content. The volatile loss measured in the LOI is more likely  
822 associated with the combustion of carbonates. In general, shallow pedoliths in the  
823 arid zone do not show much variability in pedolith thickness nor do they provide  
824 insight into the influence of physical or chemical properties on GPR signals.

825 In Santa Gracia (Figs 6, and 7; Figs S4 to S6), the field-observed pedolith  
826 thicknesses of the different pedons are more variable than in Pan de Azúcar.  
827 Although the 500 MHz and 1000 MHz GPR envelopes indicate changes at depth,  
828 the physical and chemical properties observed with depth show only a few distinct  
829 changes implying that the pedolith thickness cannot easily be determined using only  
830 physical or chemical properties. The PCA indicates that most of the variance in PC1  
831 is explained by the envelope signals, bulk density, and CIA whereas PC2 is  
832 dominated by clay content and  $\tau$  of Na and Zr. The clay content does not seem  
833 to be a dominant factor for the envelope signal, but rather represents a complex  
834 interaction between physical and chemical property changes that cannot be  
835 disentangled with available data. It appears that the second energy interval in the  
836 1000 MHz envelope may agree with the observed pedolith thickness in Santa  
837 Gracia, and (in contrast to the Pan de Azúcar location) the first maximum in the 500  
838 MHz envelope does agree with the observed pedolith thickness. These  
839 observations again underscore that for different locations with variable regolith  
840 type, vegetation, and physical and chemical properties local calibration between  
841 pedons and GPR data are required.

842 The determination of pedolith thickness from GPR data in La Campana is as  
843 difficult as in the previous settings (Figs 8, and 9; Figs S7 to S9). Field observations  
844 indicate relatively thick transition zones from the B to C horizons, and some physical  
845 properties vary only weakly with depth. As a result, the determination of pedolith  
846 thickness with physical and chemical properties is difficult, despite the moderate to

Deleted: and physical

Deleted: S3

Deleted: soil

Deleted: soil

Deleted: as soils

Deleted: the

Deleted: soils

Deleted: soil

Deleted: Fig.

Deleted: , 7

Deleted: Fig.

Deleted: soil

Deleted: soil

Deleted: soil

Deleted: soil

Deleted: soil

Deleted: soil

Deleted: Fig.

Deleted: , 9

Deleted: Fig.

Deleted: The field

Deleted: large

Deleted: for

Deleted: the

Deleted: horizon

Deleted: soil

873 strong correlation of 500 MHz GPR envelopes with derivatives of physical and  
874 chemical properties. Whereas PC1 explains much of the variance in terms of bulk  
875 density, LOI, Tau  $\tau$  of Na and Zr, and volumetric strain  $\epsilon_{strain}$ , the PC2 consists out  
876 of the envelopes, CIA, pH, and CEC. Chemical properties seem to have a  
877 considerable influence on GPR signals in this setting. In La Campana, the first  
878 energy interval in the 500 MHz envelope is interpreted to reflect the presence of the  
879 stone layer whereas the second energy interval seems to match the observed  
880 pedolith thickness. Given these uncertainties in local conditions, a clear  
881 identification of pedolith thickness from GPR data is difficult, even with local  
882 calibration to a pedon.

883 Finally, in Nahuelbuta (Figs 10 and 11; Figs S10 to S12), the observed pedolith  
884 thickness in the field is the deepest of all the four study areas and reaches from 50  
885 to 100 cm. The pedolith thickness is easily identifiable based on physical properties,  
886 (e.g., bulk density, grain size variation). The derivatives of the physical properties  
887 correlate moderately with the available 500 MHz envelope (Table 3). Furthermore,  
888 the chemical properties correlate weakly with the GPR envelope. The variance is  
889 strongly explained by PC1 containing physical properties (e.g., bulk density, clay  
890 content, LOI) and less by PC2 including chemical properties (e.g., pH, Tau  $\tau$  of Na  
891 and Zr). Even though changes in properties are more pronounced in Nahuelbuta  
892 than in the drier locations, a clear correlation between maximums in the 500 MHz  
893 energy envelope and pedolith thickness is not present. The second energy interval  
894 of the 500 MHz envelope best agrees with the observed pedolith thickness.  
895 However, due to local inhomogeneities caused by intense vegetation, every pedon  
896 and its attributed GPR envelope looks different.

897 In summary, the 500 and 1000 MHz envelopes at point locations have the  
898 potential to be used to determine pedolith thickness. But the clarity with which this  
899 can be done is variable and requires calibration to local pedons. Even with local  
900 calibration, the relationships are not always clear (e.g., Fig. 8). Physical and  
901 chemical properties with depth exert a complex influence on measured GPR signals.  
902 If a certain combination of physical and chemical properties is dominant in one

Deleted: PC1 is explained by

Deleted: variance in

Deleted: is dominated by

Deleted: of

Deleted: previously described

Deleted: soil

Deleted: soil

Deleted: Fig.

Deleted: , 11

Deleted: Fig.

Deleted: soil

Deleted: soil

Deleted: .

Deleted: envelops

Deleted: so

Deleted: soil

Deleted: soil

Deleted: look

Deleted:

Deleted: soil

Deleted: ,

Deleted: interplay

925 setting, another combination may influence the measured GPR signal in another.  
926 For example, whereas clay content correlations are moderately positive with GPR  
927 envelopes in the dry area of Pan de Azúcar, the relationship is weaker at more  
928 southerly latitudes and is moderately negatively correlated in Nahuelbuta. Other  
929 physical properties (e.g., bulk density, LOI) only correlate well with the envelopes in  
930 the southernmost study area of Nahuelbuta. The more pronounced correlation of  
931 bulk density and LOI with the envelope signal can be attributed to the abundance of  
932 organic matter in the regolith. The presence of organic matter influences not only  
933 bulk density and LOI but also CEC and pH (all organic matter related variables).  
934 Analysis of the PCA results in light of organic matter variations identifies the  
935 following variables as being best explained from north to south: (1) in Pan de  
936 Azúcar: the GPR envelope, clay content, and CIA are most closely related; (2) in  
937 Santa Gracia: the GPR envelope, bulk density, and CIA are most closely related;  
938 (3) in La Campana: the GPR envelope, bulk density, organic matter related variables  
939 are related; and (4) in Nahuelbuta: the organic matter related variables, bulk density,  
940 and GPR envelope are most closely related.

Deleted: .

941 Thus, the influence of vegetation and the continuous addition of organic matter  
942 to regolith properties influencing GPR signals are strengthen from north to south.  
943 Therefore, which GPR frequency works best for the individual study area (due to  
944 different physical and chemical properties) needs to be investigated with information  
945 from point locations/pedons. For the arid Pan de Azúcar and semi-arid Santa Gracia  
946 we suggest using the 1000 MHz frequency (or higher), whereas for the  
947 Mediterranean climate setting of La Campana and temperate Nahuelbuta the 500  
948 MHz frequency proved better. Improvements in our approach to determine pedolith  
949 thickness from GPR data might be possible by applying multifrequency GPR  
950 techniques, which are freed from antenna effects by fusion of different frequency  
951 measurements (e.g., De Coster and Lambot, 2018). Nevertheless, the point  
952 information of pedolith thickness has the potential to be up-scaled to hillslopes in  
953 some settings using GPR transects after local calibration is conducted.

Deleted: what

Deleted: soil

Deleted: soil

954

959 **5.2 Up-scaling to hillslopes**

960 Here we use insights gained from comparisons between GPR and point  
961 locations to extrapolate the pedolith thickness along the hillslope GPR profiles (Figs  
962 2 and 3). Our efforts here complement previous work by Dal Bo et al., (2019) by  
963 adding 25 new GPR profiles that cover a larger geographic region. The up-scaling  
964 is carried out using a combination of amplitude and envelope depth-converted  
965 profiles. To do this up-scaling, we calculated the envelope along each profile. Then,  
966 using the known pedolith depth data from all pedons in one study area, this interface  
967 was estimated along the profiles by searching for the corresponding signal in the  
968 envelope at every meter. Even though the information of three-point locations is at  
969 the lower limit, the combination of field observations with GPR transects allows  
970 estimation of the lateral variability of pedolith thickness over hillslopes. However, the  
971 complications which frequency of GPR antenna to use for analysis (Dal Bo et al.,  
972 2019) in addition to what envelope interval to select (section 5.1) requires careful  
973 up-scaling of the pedolith thickness to hillslopes.

974 In Pan de Azúcar (Fig. 12; Fig. S14) the observed B to C horizon transition at  
975 point locations is typically between ~14 to 50 cm. No clear pedolith thickness could  
976 be determined based on GPR profiles. Nevertheless, pedolith thicknesses identified  
977 from 1000 MHz GPR envelopes seem to be relatively homogeneous over the entire  
978 S-facing transect with an average value of 25 ±3 cm (Table 1). In contrast, the N-  
979 facing transect indicates a thinner pedolith uphill than downhill where it reaches a  
980 maximum depth of ~50 cm (Fig. S14). In Santa Gracia (Fig. 13; Figs S15 to 17), the  
981 pedolith thicknesses from point locations/pedons in the S-facing transect increases  
982 downslope and ranges between 20 to 60 cm (Table 1). The pedolith thickness based  
983 on the 1000 MHz GPR envelope at the top-slope position (SGPED20) decreases  
984 first downhill and then increases again, thereby demonstrating laterally variability  
985 down the hillslope. The pedolith thickness in the mid-slope position (SGPED40) is  
986 variable and reaches from 25 to 50 cm. At the toe-slope position (SGPED60) a  
987 mostly constant thickness of 30 cm is identified. In the N-facing transect almost no  
988 variability in pedolith thickness (~25 cm) is observed. Although the pedolith

Deleted: soil

Deleted: Fig.

Deleted: ,

Deleted: soil

Deleted: soil

Deleted: given

Deleted: mentioned in section 5.1 (e.g.,

Deleted: and

Deleted: use) the

Deleted: and

Deleted: indicated soil

Deleted: need to be treated with care

Deleted: Supplementary

Deleted: soil

Deleted: soil

Deleted: 2

Deleted: soil

Deleted: ¶

Deleted: Supplementary Fig.

Deleted: soil

Deleted: 2

Deleted: soil

Deleted: along

Deleted: soil

Deleted: soil

Deleted: Even so

Deleted: soil



1068 the pedolith, and could therefore be used to extrapolate point-scale ground-truth  
1069 information over the profile scale.

1070 In summary, the application of GPR envelopes to determine pedolith thicknesses  
1071 provides more information than pedolith thicknesses determined from GPR  
1072 transects alone where in some cases no clear reflections may be visible. Generally,  
1073 the findings of this study agree with the findings of Bernhard et al. (2018) as well as  
1074 Dal Bo et al., (2019). Pedolith thicknesses increase from north to south in latitude.  
1075 Due to the increase in vegetation amount pedolith thicknesses are also less  
1076 homogenous from increasing latitude (north to south). Due to the increasing  
1077 heterogeneity in pedolith thickness, no clear trend in increasing pedolith thickness  
1078 from top- to toe-slope is easily detectable. Only in Santa Gracia, the constantly thin  
1079 pedoliths at the S-facing top-slope are in contrast to the thicker and more variable  
1080 pedolith thickness in the mid-slope position. Bernhard et al., (2018) describe an  
1081 increase of the A to BC horizon from top- to toe-slope in the S-facing hillslope. In  
1082 addition, a clear difference between pedolith thickness from S- and N-facing slopes  
1083 could not be detected for the more heavily vegetated study areas in the south.  
1084 Again, only in Santa Gracia with little vegetation an expected difference in pedolith  
1085 thickness between S- and N-facing slopes was detectable. The increase in  
1086 vegetation under increasing precipitation rates causes not only more heterogenous  
1087 pedolith depths, but also stabilization of hillslopes (e.g., Langbein and Schumm,  
1088 1958; Schmid et al., 2018; Starke et al., 2020).

### 1090 5.3 Comparison to previous work and study caveats

1091 Geophysical studies focusing on the critical zone are a relatively new topic and  
1092 have gained emphasis in the past decades (e.g., Parsekian et al., 2001). The results  
1093 presented in this study complement a range of previous studies. Previous studies  
1094 have used near surface geophysical methods to non-invasively measure subsurface  
1095 properties and structures of the regolith and help to characterize critical zone related  
1096 processes in the shallow subsurface (e.g., Scott and Pain, 2009). In this study, we  
1097 focused in particular on deploying surface ground penetrating radar (GPR). The

**Deleted:** soil

**Deleted:** ¶  
**5.3 Changes of soil thickness with hillslope position, aspect, and latitude**¶  
The soil thickness imaged with

**Deleted:** over hillslope transects reflect mainly physical properties, but also chemical properties (e.g., CIA, τ). This approach gives the opportunity

**Deleted:** study non-invasively possible changes in soil thickness over hillslope position, aspect, and latitude (Fig. 12 to 15; Fig. S14 to S24; Table 2). Here we summarize any regional trends in soil thickness between the four study areas and different aspect (N- vs. S-facing) hillslopes (Fig. 2).¶  
Soil thickness in a catena that develop under comparable climate and on similar lithologies are expected to increase downhill (e.g., Birkeland, 1999). From the top- to toe-slope position along a catena the potential for physical erosion decreases downslope due to decreasing physical potential whereas the potential for deposition increases. In Pan de Azúcar, the soil thickness based on the GPR envelopes in the S-facing hillslope are constant, whereas the N-facing hillslope indicates soil thickness increasing from top- to toe-slope. The possible slight increase in soil thickness from top- to toe-slope can be explained by low denudation rates due to very low precipitation rates in Pan de Azúcar. In Santa Gracia, the constantly thin soils

**Deleted:** soil

**Deleted:** In Santa Gracia, precipitation and minor vegetation cover may cause the increase of the soil thickness downslope as well as the variable soil thickness in the mid-slope position. In La Campana, the soil thickness based on GPR envelopes is highly variable. Bernhard et al., (2018) observed the thickest soil also in the mid-slope position, describe a disturbed hillslope with recent erosion events (e.g., possibly due to a past fire and temporary mobilization of sediment). Therefore, the S-facing hillslope in La Campana is a disturbed system and therefore difficult to laterally extrapolate horizons. Due to the differences in soil thickness information from the different methods, soil thickness changes in hillslopes from Nahuelbuta are not further considered.¶  
In the southern hemisphere the N-facing hillslope is expected to be slightly warmer (higher solar irradiation) and drier (due to higher evaporation) than the S-facing hillslope (e.g., Anderson

**Moved down [3]:** et al., 2013).

**Deleted:** These differences in available soil moisture could potentially lead to different vegetation and soil thickness. In Pan de Azúcar, the soil thickness of the S- and N-facing mid-slope positions cannot be attributed to differences in vegetation cover because it is absent from both the N- and S-facing slopes. In Santa Gracia, however, the thicker soil in the S-facing mid-slope position than in N-facing position can either [4]

**Moved up [1]:** Oeser et al., 2018).

**Deleted:** Different vegetation on S-facing and N-facing slope positions in La Campana could explain the higher variability in soil thickness in the S-facing mid-slope positions (35 to 70 cm) than the N-facing hillslope (50 to 60 cm). However, the aspect-related differences in La Campana may represent local ... [5]

**Deleted:** the

**Deleted:** due to increasing precipitation rates

1192 [electromagnetic properties of the subsurface affect the propagation \(i.e. velocity\),](#)  
1193 [attenuation \(i.e. the energy loss\), and reflectivity of the electromagnetic waves \(e.g.,](#)  
1194 [Jol, 2009\).](#) [The electromagnetic wave velocity and attenuation can be linked to the](#)  
1195 [dielectric permittivity and electrical conductivity of the subsurface, respectively.](#)  
1196 [Previous work provides examples of environments, where GPR is suitable for](#)  
1197 [mapping subsurface properties. These include karst areas, where structures in the](#)  
1198 [regolith have been identified up to the bedrock interface \(e.g., Estrada-Medina et](#)  
1199 [al., 2010; Fernandes Jr. et al., 2015; Carriere et al., 2013\), volcanic environments](#)  
1200 [\(e.g., Gomez et al., 2012; Ettinger et al., 2014\), and dry environments \(e.g., Bristow](#)  
1201 [et al., 2007; Harari, 1996\) as generally these regimes are characterized by low clay](#)  
1202 [and water content. The primary new contribution of this study with respect to existing](#)  
1203 [regolith studies is the comparison of GPR data to a wide range of physical and](#)  
1204 [chemical properties that are commonly interpreted in projects studying surface](#)  
1205 [processes.](#)

1206 [Previous work has highlighted the primary factors that GPR data can be sensitive](#)  
1207 [to, and we briefly discuss these in the context of caveats associated with our work.](#)  
1208 [Important factors that influence GPR data are the presence of water, solute content,](#)  
1209 [and conductive materials such as clay \(e.g., Scott and Pain, 2009; Huisman et al.,](#)  
1210 [2003\). In particular, clay as a highly conductive material has a significant impact on](#)  
1211 [GPR signal as it affects the permittivity and the electrical conductivity at the same](#)  
1212 [time \(e.g., Daniels, 2004\). With increasing amounts of clay in the subsurface, the](#)  
1213 [signal penetrating is decreased due the increased attenuation of the waves.](#)  
1214 [However, this behavior can be used to identify fine material in the subsurface, since](#)  
1215 [in GPR profiles clay layers could be identified starting from spatial differences in](#)  
1216 [signal penetration \(e.g., Gómez-Ortiz et al., 2010; De Benedetto et al., 2010; Tosti](#)  
1217 [et al., 2013\).](#) [Furthermore, particle size beyond just clay content also plays a major](#)  
1218 [role in GPR measurements, as the closer the particle size is to the wavelength of](#)  
1219 [the emitted electromagnetic waves, the stronger are the reflections generated by](#)  
1220 [these particles that can be seen in the detected signals \(e.g., Jol, 2009\). In this](#)

Moved (insertion) [3]

Moved (insertion) [2]

**Deleted:** Hillslope denudation rates derived from *in situ*-produced cosmogenic nuclides increase from Pan de Azúcar to La Campana and slightly decrease for Nahuelbuta (Schaller et al., 2018; Oeser et al., 2018). Increasing soil thickness generally diminishes soil production rates (e.g., Heimsath et al., 1997) which under steady-state conditions equal hillslope denudation rates.¶

1228 [study, we incorporated clay content into our PCA and correlation analysis to identify](#)  
1229 [if, and by how much, it may influence GPR observations.](#)

1230 [Previous studies have also documented how mineralogical variations with depth](#)  
1231 [influence GPR signals. For example, the presence of minerals such as iron and](#)  
1232 [aluminum oxides/hydroxides can play an important role in limiting the depth of](#)  
1233 [penetration for GPR waves \(e.g., Čeru et al., 2018\) as iron-oxides have been linked](#)  
1234 [with variations of relative permittivity, which might have in turn a considerable effect](#)  
1235 [in the propagation of the GPR signals and effect the interpretation \(e.g., Van Dam](#)  
1236 [et al., 2003; Van Dam and Schlager, 2000; Havholm et al., 2003\). Other studies](#)  
1237 [showed that with increasing mafic mineral content in the subsurface, GPR signal](#)  
1238 [attenuation is higher \(e.g., Breiner et al., 2011\). The presence of clay lenses in the](#)  
1239 [regolith, alongside the layering, can influence the preferential flow path for regolith](#)  
1240 [water, which can enhance reflectivity of the surfaces and therefore produce](#)  
1241 [detectable reflections \(e.g., Zhang et al., 2014\). In this study, mineralogical](#)  
1242 [variations with depth in the pedons were not available for comparison to our GPR](#)  
1243 [data. However, we note that many of the processes described above may be](#)  
1244 [responsible for the subsurface reflectors observed in Figures 12 to 15, and the fairly](#)  
1245 [uniform granitoid composition of the different study areas means that mineralogical](#)  
1246 [variations along any given hillslope profile are likely minimal and not a dominant](#)  
1247 [source of signal in our GPR data.](#)

1248 [The presence of volumetric water limits GPR signal penetration, with an](#)  
1249 [increasing effect at higher frequencies \(e.g., Utsi, 2017; Miller et al., 2002\). GPR](#)  
1250 [techniques have been used in the past two decades as a tool to detect water content](#)  
1251 [variations in the subsurface as it has a strong effect on the dielectric permittivity](#)  
1252 [\(e.g., Klotzsche et al., 2018\). In compact regoliths, where the volumetric water](#)  
1253 [content is small, it has been shown that the bulk density has an important effect on](#)  
1254 [the wave velocity, which is positively correlated \(Wang et al., 2016\). When solutes](#)  
1255 [are present in the groundwater, the electrical conductivity of the medium increases,](#)  
1256 [generating more signal loss, and therefore increasing wave attenuation \(e.g.,](#)  
1257 [Benedetto and Palewski, 2015\). One shortcoming of our study is that no information](#)

1258 [about subsurface water content within the pedon depth profiles was available for](#)  
1259 [comparison to GPR observations as we did with the regolith physical and chemical](#)  
1260 [properties. The depth varying chemical weathering indices we present \(e.g., CIA,](#)  
1261 [Tau, Fig. 4 to 10\) would not be expected to correlate with present-day water content](#)  
1262 [as these weathering indices developed over the timescale of regolith development](#)  
1263 [\(millennia and longer\). Nevertheless, we find that out of the four study areas](#)  
1264 [investigated, the present-day water content appears to influence the GPR signals](#)  
1265 [and interpretations presented here only in the southernmost and wettest study area](#)  
1266 [Nahuelbuta. As a result, the subsurface correlations between the GPR envelopes](#)  
1267 [and physical or chemical properties at this location are likely influenced, to an](#)  
1268 [unknown degree, by regolith water content. The exclusion of regolith water content](#)  
1269 [in our analysis may very well be a reason why we are not able to explain the full](#)  
1270 [radar signature. Although without the inclusion of this data, peaks in the radar](#)  
1271 [envelopes were still interpretable when compared to available physical and](#)  
1272 [chemical property variations with depth. Thus, although the inclusion of regolith](#)  
1273 [water content would be preferred, the omission of it does not negate the observed](#)  
1274 [signals we were able to interpret.](#)

1275 [In locations, where the aforementioned regolith properties are not dominant, GPR](#)  
1276 [can be used as a tool to identify structures and layering in both sediments \(e.g.,](#)  
1277 [Bristow and Jol, 2003\) and regoliths, where interfaces ranging from the regolith-](#)  
1278 [bedrock limit to the B horizon have been identified due to changes in the dielectric](#)  
1279 [permittivity \(e.g., Yoder et al., 2001; Lambot et al., 2006\). In particular Zhang et al.](#)  
1280 [\(2018\) showed the potential of mapping regolith layering in grasslands obtaining](#)  
1281 [differences between GPR reflections and real regolith layer depth within 3 cm. In](#)  
1282 [many situations, the interplay between different regolith properties make it difficult](#)  
1283 [to understand the subsurface architecture without validation through regolith](#)  
1284 [samples, as shown by Orlando et al. \(2016\) in the Rio Icacos watershed \(Puerto](#)  
1285 [Rico\), where the stress regime, climate, and lithology are controlling the structures](#)  
1286 [visible in GPR profiles. In comparing the previous studies to this one, we note that](#)  
1287 [‘in general’ the results of this study were able to identify subsurface regolith structure](#)

1288 [and explain them, in many cases, with available physical and chemical properties.](#)  
1289 [However, the complexity in GPR signals observed necessitates having pedons for](#)  
1290 [local calibration when comparing to regolith weathering indices.](#)  
1291

Formatted: Indent: First line: 0 cm

## 1292 **6 Conclusions**

1293 [Pedolith](#) thickness and [physical and chemical](#) properties are investigated in four  
1294 study areas along a climate and vegetation gradient. [This gradient spans from arid](#)  
1295 [and Mediterranean to temperate humid conditions.](#) The visually observed transition  
1296 from [the](#) mobile [pedolith](#) to immobile [saprolite](#) coincides with one or more changes  
1297 in measured physical and chemical properties in each study area. These physical  
1298 and chemical properties in turn, influence return signals generated by Ground  
1299 Penetrating Radar (GPR) in the [regolith](#), but no systematic trend is visible for which  
1300 physical or chemical properties correlate with GPR based observations of [pedolith](#)  
1301 thickness. Given this, the measurements and interpretation of GPR signals for  
1302 systematically identifying subsurface changes in physical and chemical properties  
1303 is not straightforward and differs for each study area. In general, the better  
1304 developed the [pedolith](#) the better the correlation of GPR signals from point locations  
1305 with physical and chemical [regolith](#) properties. We note that [choosing the](#) GPR  
1306 antenna [frequency that](#) is best suited for identifying [pedolith](#) thickness is difficult,  
1307 and calibration to local point locations (e.g., pedons) is always required.  
1308 [Furthermore, we found that the higher-frequency \(1000 Mhz\) antenna worked best](#)  
1309 [for imaging pedolith layers for comparison to chemical indicators in the arid and](#)  
1310 [semi-arid study areas \(Pan de Azuár and Santa Gracia\). In contrast, the lower](#)  
1311 [frequency antenna \(500 Mhz\) worked better in the Mediterranean and temperate](#)  
1312 [study areas \(La Campana and Nahuelbuta\) for imaging pedolith structure and for](#)  
1313 [comparison to chemical observations.](#)  
1314

Deleted: Soil

Deleted: soil

Deleted: saprolite

Deleted: -

Deleted: sub-surface

Deleted: soil

Deleted: soil

Deleted: soil

Deleted: what frequency

Deleted: soil

Deleted: .

Deleted: However, after local calibration between GPR signals

Deleted: point locations is conducted, information of soil thickness from point locations can be up-scaled to hillslope transects with care.

1331 **Acknowledgement**

1332 We would like to thank CONAF and all the Park Rangers for the possibility of working  
1333 in the natural parks, for providing access to the sample locations, and help inside  
1334 the National Parks. [We also thank C. Pain, L. Worrall, and the topical editor D.  
1335 Dunkerley for their reviews of an earlier version of the manuscript.](#) We acknowledge  
1336 support from the German Science Foundation (DFG) priority research program  
1337 SPP-1803 “EarthShape: Earth Surface Shaping by Biota” (grants KR 3725/1-1,  
1338 SCHA 1690/3-1, [and EH329/17-2](#)). RD was supported by a DFG Emmy Noether  
1339 grant (DR 822/3-1).

1340

1341

1342

1343

Deleted: sub

Deleted: and

1346 **References:**

- 1347 [Aranha, P.R.A., Augustin, C.H.R.R., and Sobreira, F.G. The use of GPR for](#)  
1348 [characterizing underground weathered profiles in the sub-humid tropics, Journal](#)  
1349 [of Applied Geophysics, 49, 195-210, 2002.](#)
- 1350 [Ardekani, M.R., Neyt, X., Benedetto, D., Slob, E., Wesemael, B., Bogaert, P.,](#)  
1351 [Craeye, C., and Lambot, S. Soil moisture variability effect on GPR data,](#)  
1352 [Proceedings of the 15th International Conference on Ground Penetrating](#)  
1353 [Radar, Brussels, 214-217, doi: 10.1109/ICGPR.2014.6970416, 2014.](#)
- 1354 Armesto, J.J., Vidiella, P.E., and Gutierrez, J.R. Plant communities of the fog-free  
1355 coastal desert of Chile: plant strategies in a fluctuating environment, Revista  
1356 Chilena de Historia Natural, 66, 271-282, 1993.
- 1357 [Benedetto, A., and Pajewski, L. Civil engineering applications of ground penetrating](#)  
1358 [radar, Springer, 2015.](#)
- 1359 Bernhard, N., Moskwa, L.-M., Oeser, R., von Blanckenburg, F., Boy, H., Brucker,  
1360 E., Dippold, M., Ehlers, T.A., Fuentes-Espoz J.P., Godoy, R., Köster, M., Osses,  
1361 P., Paulino, L., Schaller, M., Scholten, T., Seguel, O., Spielvogel, S., Spohn, M.,  
1362 Stock, S., Stroncik, N., Uebernickel, K., Wagner, D., Kühn, P.: Pedogenic and  
1363 microbial interrelations to regional climate and local topography: New insights  
1364 from a climate gradient (arid to humid) along the Coastal Cordillera of Chile,  
1365 Catena, 170, 335-355, 2018.
- 1366 [Braun, J.-J., Desclotres, M., Riotte, J., Fleury, S., Barbiero, L., Boeglin, J.-L.,](#)  
1367 [Violette, A., Lacarce, E., Ruiz, L., Sekhar, M., Mohan Kumar, M.S.,](#)  
1368 [Subramanian, S., and Dupre, B. Regolith mass balance inferred from combined](#)  
1369 [mineralogical, geochemical and geophysical studies: Mule Hole gneissic](#)  
1370 [watershed, South India, Geochimica et Cosmochimica Acta, 73, 935-961, 2009.](#)
- 1371 [Breiner, J.M., Doolittle J.A., Horton R., and Graham R.C. Performance of ground-](#)  
1372 [penetrating radar on granitic regoliths with different mineral composition, Soil](#)  
1373 [Science, 176, 435-440, 2011.](#)
- 1374 Brimhall, G.H., and Dietrich, W.E. Constitutive mass balance relations between  
1375 chemical composition, volume, density, porosity, and strain in metasomatic  
1376 hydrochemical systems: Results on weathering and pedogenesis, Geochimica  
1377 et Cosmochimica Acta, 51 (3), 567-587, 1987.
- 1378 Brimhall, G.H., Alpers, C., and Cunningham, A.B. Analysis of supergene ore-forming  
1379 processes using mass balance principles, Economic Geology, 80, 1227-1254,  
1380 1985.
- 1381 [Bristow, C.S., and Jol, H.M. An introduction to ground penetrating radar \(GPR\) in](#)  
1382 [sediments, Geological Society, London, Special Publications 211, 1, 1-7, 2003.](#)
- 1383 [Bristow, C.S., Jones, B.G., Nanson, G.C., Hollands, C., Coleman, M., and Price,](#)  
1384 [D.M. GPR surveys of vegetated linear dune stratigraphy in central Australia:](#)  
1385 [Evidence for linear dune extension with vertical and lateral accretion, Special](#)  
1386 [Papers- Geological Society of America, 432, 19, 2007.](#)
- 1387 [Carriere, S.D., Chalikakis, K., Senechal, G., Danquigny C., and Emblanch C.](#)  
1388 [Combining electrical resistivity tomography and ground penetrating radar to](#)

**Deleted:** Abdi, H., and Williams, L.J. Principal component analysis, Wiley interdisciplinary reviews: computational statistics 2, 433-459, 2010.¶

**Deleted:** Anderson, S.P., Anderson, S.P., and Tucker, G.E. Rock damage and regolith transport by frost: An example of climate modulation of the geomorphology of the critical zone, Earth Surface Processes and Landforms, DOI: 10.1002/esp.3330, 2013.¶

**Formatted:** EndNote Bibliography, Line spacing: single

**Formatted:** Line spacing: single

**Formatted:** Line spacing: single

**Deleted:** Birkeland, P.W. Soils and Geomorphology, Oxford University Press, New York, 1999.¶

**Formatted:** Normal (Web), Indent: Left: 0 cm, Hanging: 0.63 cm, Line spacing: single

**Deleted:** Bro, R., and Smilde, A.K. Principal component analysis, Analytical Methods, 6, 2812-2831, 2014.¶

1401 [study geological structuring of karst unsaturated zone, Journal of Applied](#)  
1402 [Geophysics, 94, 31-41, 2013.](#)  
1403 [Čeru, T., Dolonec, M., and Gosar, A. Application of Ground Penetrating Radar](#)  
1404 [Supported by Mineralogical-Geochemical Methods for Mapping Unroofed Cave](#)  
1405 [Sediments, Remote Sensing 10, 4, 639, 2018.](#)  
1406 Chadwick, O.A., Brimhall, G.H., and Hendricks, D.M. From a black to a gray box - a  
1407 mass balance interpretation of pedogenesis, *Geomorphology*, 3, 369-390,  
1408 1990.  
1409 Dal Bo, I., Klotzsche, A., Schaller, M., Ehlers, A.T., Kaufmann, M.S., Fuentes-  
1410 Espoz, J.P., Vereecken, H., van der Kruk, J. Geophysical imaging of regolith in  
1411 landscapes along a climate and vegetation gradient in the Chilean Coastal  
1412 Cordillera, *Catena*, 180, 146-159, 2019.  
1413 [Daniels, D.J. Ground penetrating radar, IEE Radar, Sonar, Navigation and Avionics](#)  
1414 [Series, The Institution of Electrical Engineers, 15, 2004.](#)  
1415 [De Benedetto, D., Castrignano, A., Sollitto, D., and Modugno, F. Spatial relationship](#)  
1416 [between clay content and geophysical data, Clay Minerals 45, 2, 197-207, 2010.](#)  
1417 De Coster, A., and Lambot, S. Fusion of Multifrequency GPR Data Freed From  
1418 Antenna Effects, *Journal of Selected Topics in Applied Earth Observations and*  
1419 *Remote Sensing*, 11 (2), 664-674, 2018.  
1420 Doolittle, J.A., and Collins, M.E. Use of soil information to determine application of  
1421 ground penetrating radar. *Journal of Applied Geophysics*, 33 (1-3), 101-105,  
1422 1995.  
1423 Doolittle, J.A., Minzenmayer, F.E., Waltman, F.W., Benham, E.C., Tuttle, J.W., and  
1424 Peaslee, S.D. Ground-penetrating radar soil suitability map of the conterminous  
1425 United States, *Geoderma*, 141, 416-421, 2007.  
1426 [Estrada-Medina, H., Tuttle, W., Graham, R.C., Allen, M.F., and Jimenez-Osornio, J.](#)  
1427 [Identification of Underground Karst Features using Ground-Penetrating Radar in](#)  
1428 [Northern Yucatan, Mexico, Vadose Zone Journal, 9, 3, 653-661, 2010.](#)  
1429 [Ettinger, S., Manville, V., Kruse, S., and Paris, R. GPR-derived architecture of a](#)  
1430 [labor-generated fan at Cotopaxi volcano, Ecuador, Geomorphology, 213, 225-](#)  
1431 [239, 2014.](#)  
1432 [Fernandes Jr., A.L. Medeiros, W.E., Bezerra, F.H.R., Oliveira Jr., J.G., and Cazarin,](#)  
1433 [C.L. GPR investigation of karst guided by comparison with outcrop and](#)  
1434 [unmanned aerial vehicle imagery, Journal of Applied Geophysics, 112, 268-278,](#)  
1435 [2015.](#)  
1436 Gerber, R., Felix-Henningsen, P., Behrens, T., and Scholten, T. Applicability of  
1437 ground-penetrating rader as a tool for nondestructive soil-depth mapping on  
1438 Pleistocene slope deposits, *Journal of Plant Nutrition and Soil Science*, 173 (2),  
1439 173-184, 2010.  
1440 [Gomez, C., Kataoka, K.S., and Tanaka, K. Large-scale internal structure of the](#)  
1441 [Sambongi Fan-Towada Volcano, Japan: Putting the theory to the test using PGR](#)  
1442 [on volcanoclastic deposits, Journal of volcanology and geothermal research,](#)  
1443 [229, 44-49, 2012.](#)

Formatted: Line spacing: single

Formatted: Line spacing: single

Formatted: Line spacing: single

1444 [Gómez-Ortiz, D., Martin-Crespo, T., Martin-Velazquez, S., Martinez-Pegan, P.,](#)  
1445 [Higuera, H., and Manzana, M. Application of ground penetrating radar \(GPR\)](#)  
1446 [to delineate clay layers in wetlands. A case study in the Soto Grande and Soto](#)  
1447 [Chico watercourses, Donana \(SW Soain\), Journal of Applied Geophysics, 72, 2,](#)  
1448 [107-113, 2010.](#)

1449 Green, A.G. Applications of 3-D georadar methods to diverse environmental and  
1450 engineering problems, Progress in Environmental and Engineering Geophysics,  
1451 edited by Chao, C. and Jianghai, X., Science Press USA, 220-226, 2004.

1452 Guo, L., Chen, J., Cui, X., Fan, B., and Lin, H. Application of ground penetrating  
1453 radar for coarse root detection and quantification: a review, Plant Soil, 362, 1-  
1454 23, 2013.

1455 Guo, L., Mount, G.J, Hudson, S., Lin, H., and Levia, D. Pairing geophysical  
1456 techniques helps understanding of the near-surface Critical Zone: Visualization  
1457 of preferential routing of stemflow along coarse roots. Geoderma, 357, 113953,  
1458 2020.

1459 [Harari, Z. Ground-penetrating radar \(GPR\) for imaging stratigraphic features and](#)  
1460 [groundwater in sand dunes. Journal of Applied Geophysics, 36, 1, 43-52, 1996.](#)

1461 [Havholm, K.G., Bergstrom, N.D., Jol, H.M., and Running, G.L. GPR survey of a](#)  
1462 [Holocene aeolian/fluvial/lacustrine succession, Lauder Sandhills, Manitoba,](#)  
1463 [Canada, Geological Society, London, Special Publication 211, 47-54, 2003.](#)

1464 Heimsath, A.M., Dietrich, W.E., Nishiizumi, K., and Finkel, R.C. The soil  
1465 production function and landscape equilibrium, Nature, 388, 358-361, 1997.

1466 Heimsath, A.M., Dietrich, W.E., Nishiizumi, K., and Finkel, R.C. Cosmogenic  
1467 nuclides, topography, and the spatial variation of soil depth, Geomorphology,  
1468 27, 151-172, 1999.

1469 Hilgard, E.W. Soils: Their Formation, Properties, Compositions and Relations to  
1470 Climate and Plant Growth in the Humid and Arid Regions, The Macmillan  
1471 Company, New York, 1914.

1472 Holbrook, W.S., Riebe, C.S., Elwaseif, M., Hayes, J.L., Vasler-Reeder, K., Harry,  
1473 D.L., Malazian, A., Dosseto, A., Hartsough, P.C., and Hopmans, W.  
1474 Geophysical constraints on deep weathering and water storage potential in the  
1475 Southern Sierra Critical Zone Observatory. Earth Surface Processes and  
1476 Landforms, 39, 366-380, 2014.

1477 Hruska, J., Cermak, J., and Sustek, S. Mapping tree root system with ground-  
1478 penetrating radar. Tree Physiology, 19, 125-130, 1999.

1479 [Huisman, J.A., Hubbard, S.S., Annan, P.A. Measuring soil water content with](#)  
1480 [ground penetrating radar: A review, Vadose Zone Journal, 2, 476-491,](#)  
1481 [doi:10.2136/vzj2003.4760, 2003.](#)

1482 [IUSS Working Group WRB. World reference base for soil resources 2014, update](#)  
1483 [2015. Prepared by Schad P, van Huyssteen C, Micheli E. 192 pp. World Soil](#)  
1484 [Resources Reports No. 106, FAO, Rome. 2015.](#)

1485 Jenny, H. Factors of Soil Formation: A System of Quantitative Pedology, Dover  
1486 Publications, New York, 1994.

Formatted: Normal, Indent: Left: 0 cm, Hanging: 0.63 cm,  
Line spacing: single

Formatted: Line spacing: single

Formatted: Line spacing: single

Formatted: Line spacing: single

1487 Jol, H.M. (Ed.): Ground penetrating radar: theory and applications, Elsevier Science,  
1488 Amsterdam, the Netherlands ; Oxford, United Kingdom, 2009.

1489 Kassambara, A. Practical guide to cluster analysis in R: unsupervised machine  
1490 learning, STHDA, 2017.

1491 [Klotzsche, A, Jonard, F., Looms, M.C., van der Kruk, J., and Huisman, J.A.](#)  
1492 [Measuring soil water content with ground penetrating radar: A decade of](#)  
1493 [progress, \*Vadose Zone Journal\*, 17, 1, 1-9, 2018.](#)

1494 [Lambot, S., Antoine, M., Vanclooster, M., Slob E.C.](#) Effect of soil roughness on the  
1495 [inversion of off-ground monostatic GPR signal for noninvasive quantification of](#)  
1496 [soil properties, \*Water Resources Research\*, 42, 3, 2006.](#)

1497 Langbein, W.B., and Schumm, S.A. Yield of sediment in relation to mean annual  
1498 precipitation, *Transaction American Geophysical Union*, 39, 1076-1084, 1958.

1499 Liu, J.L., and Marfurt, K.J. Instantaneous Spectral Attributes to Detect Channels,  
1500 *Geophysics*, 72, 23-31.  
1501 <http://dx.doi.org/10.1190/1.2428268>, 2007.

1502 Mellett, J.S. Ground penetrating radar applications in engineering, environmental  
1503 management, and geology, *Journal of Applied Geophysics*, 33 (1-3), 157-166,  
1504 1995.

1505 Miller, T.W., Hendrickx, J.M.H., and Borchers, B. Radar detection of burried  
1506 landmines field soils. *Vadose Zone Journal*, 3 (4). 1116-1127, 2002.

1507 Mutz, S.G., Ehlers, T.A., Werner, M., Lehmann, G., Stepanek, C., and Li, J. Where  
1508 is Late Cenozoic climate change most likely to impact denudation?, *Earth*  
1509 *Surface Dynamics*, 6, 271-301, <https://doi.org/10.5194/esurf-2017-47>, 2018.

1510 [Nesbitt, H.W., and Young, G.M.](#) [Early Proterozoic climates and plate motions](#)  
1511 [inferred from major element chemistry of lutites, \*Nature\*, 299, 215-217, 1982.](#)

1512 [Oeser, R.A., Stroncik, N., Moskwa, L.-M., Bernhard, N., Schaller, M., Canessa, R.,](#)  
1513 [van der B Rin, L., Köster, M., Brucker, E., Stock, SS., Fuentes, J.P., Godoy, R.,](#)  
1514 [Matus., F.J., Oses Pedraza, R., Osses McIntyre, P., Paulino, L., Seguel, O.,](#)  
1515 [Bader, M.Y., Boy, J., Dippold, M.A., Ehlers, T.a., Kühn, P., Kuzyakiv, Y.,](#)  
1516 [Peinweber, P., Scholten, T., Spielvogel, S., Spohn, M., Üubernickel, K.,](#)  
1517 [Tielbörger, K., Wagner, D., and von Blanckenburg, F.](#) Chemistry and  
1518 microbiology of the Critical Zone along a steep climate and vegetation gradient  
1519 in the Chilean Coastal Cordillera, *Ctena*, 170, 183-203, 2018.

1520 [Orlando, J., Comas, Z., Hynek, S., Buss, H.L., and Brantley, S.L.](#) [Architecture of the](#)  
1521 [deep critical zone in the Rio Icacos watershed \(Luquillo Critical Zone](#)  
1522 [Observatory, Puerto Rico\) inferred from drilling and ground penetrating radar](#)  
1523 [\(GPR\), \*Earth Surface Processes and Landforms\*, 41, 13, 1823-1840, 2016.](#)

1524 Parsekian, A.D., Singha, K., Minsley, B.J., Holbrook, W.S., and Slater, L. Multiscale  
1525 geophysical imaging of the critical zone, *Reviews of Geophysics*, 53, 1-26,  
1526 2015.

1527 Porder, S., Vitousek, M.P., Chadwick, O.A., Chamberlain, C. P. and Hilley, G.E.  
1528 Uplift, Erosion, and Phosphorous Limitation in Terrestrial Ecosystems,  
1529 *Ecosystems*, 10, 158-170, 2007.

Formatted: Line spacing: single

Formatted: English (US)

Formatted: Line spacing: single

Formatted: Line spacing: single

1530 Rabassa, J., and Clapperton, C.M. Quaternary glaciations of the southern Andes,  
 1531 Quaternary Science Reviews, 9, 153-174, 1990.

1532 Roering, J.J., Kirchner, J.W., and Dietrich, W.E. Hillslope evolution by nonlinear,  
 1533 slope-dependent transport: Steady state morphology and equilibrium  
 1534 adjustment timescales, Journal of Geophysical Research, 106, B8, 16499-  
 1535 16513. 2001.

1536 Roering, J.J., Marshall, J., Booth, A.M., Mort, M., and Jin, Q. Evidence for biotic  
 1537 controls on topography and soil production, Earth and Planetary Science  
 1538 Letters, 289, 183-190, 2010.

1539 Saarenketo, T. Electrical properties of water in clay and silty soils. Journal of Applied  
 1540 Geophysics, 40, 73-88, 1998.

1541 Sarkar, R., Paul, K.B., and Higgins, T.R. Impacts of soil physiochemical properties  
 1542 and temporal-seasonal soil-environmental status on ground-penetrating radar  
 1543 response. Soil Science Society of America Journal, 83, 542-554, 2019.

1544 Scarpone, C., Schmidt, M.G., Bulmer, C.E., and Knudby, A. Modelling soil thickness  
 1545 in the critical zone for Southern British Columbia, Geoderma, 282, 59–69, 2016.

1546 Schaller, M., Ehlers, T., Lang, K., Schmid, M., and Fuentes-Espoz, J. Addressing  
 1547 the contribution of climate and vegetation cover on hillslope denudation, Chilean  
 1548 Coastal Cordillera (26°–38° S), Earth and Planetary Science Letters, 489, 111-  
 1549 122, 2018.

1550 [Schmid, M., Ehlers, T.A., Werner, C., Hickler, T., and Fuentes-Espoz, J.-P. Effect](#)  
 1551 [of changing vegetation and precipitation on denudation – Part 2: Predicted](#)  
 1552 [landscape response to transient climate and vegetation cover over millennial to](#)  
 1553 [million-year timescales, Earth Surface Dynamics, 6\(4\), 859–881,](#)  
 1554 [doi:10.5194/esurf-6-859-2018, 2018.](#)

1555 [Scott, K., and Pain, C. Regolith science, Csiro Publishing, 2009.](#)

1556 Sedgwick, P. Pearson's correlation coefficient, BMJ, 345:e4483, 2012.

1557 Starke, J., Ehlers, T.A., and Schaller, M. Latitudinal effect of vegetation on erosion  
 1558 rates identified along western South America. Science, 367, 1358-1361, 2020.

1559 [Steelman, C.M., Endres, A.L., and Jones, J.P. High-resolution ground-penetrating](#)  
 1560 [radar monitoring of soil moisture dynamics: Field results, interpretation, and](#)  
 1561 [comparison with unsaturated flow model. Water Resour. Res. 48, W09538,](#)  
 1562 [doi:10.1029/2011WR011414, 2012.](#)

1563 Sucre, E.B., Tuttle, J.W., and Fox, T.R. The use of ground-penetrating radar to  
 1564 accurately estimate soil depth in rocky forest soils. Forest Science 57 (1), 59-  
 1565 66, 2011.

1566 Telford, W.M., Geldart, L.P., Sheriff, R.E. and Keys, D.A. (Eds.): Applied  
 1567 Geophysics, 2th Edition, Cambridge University Press, Cambridge, 770.  
 1568 <http://dx.doi.org/10.1017/CBO9781139167932>, 1990.

1569 Tosti, F., Patriarca, C., Slob, E., Benedetto, A., and Lambot, S. Clay content  
 1570 evaluation in soils through GPR signal processing. Journal of Applied  
 1571 Geophysics, 97, 69-80, 2013.

1572 [Utsi, E.C. Ground penetrating radar: theory and practice, Butterworth-Heinemann,](#)  
 1573 [2017.](#)

**Deleted:** Riebe, C.S., and Granger, D. Quantifying deep and near-surface chemical erosion on cosmogenic nuclides in soils, saprolite, and sediment, Earth Surface Processes and Landforms, 38, 523-533, 2013.†  
 Riebe, C.S., Hahn, W.J. and Brantley, S.L. Controls on deep critical zone architecture: a historical review and four testable hypothesis, Earth Surface Processes and Landforms, 42, 128-156, 2017.†

**Formatted:** Line spacing: single

**Formatted:** Line spacing: single

1582 [van Dam, R.L., and Schlager, W. Identifying causes of ground-penetrating radar](#)  
1583 [reflections using time-domain reflectometry and sedimentological analyses,](#)  
1584 [Sedimentology, 47, 435–449, doi: 10.1046/j.1365-3091.2000.00304.x. 2000.](#)  
1585 [van Dam, R.L., Nichol, S.L., Augustinus, P.C., Parnell, K.E., Hosking, P.L., and](#)  
1586 [McLean, R.F. GPR stratigraphy of a large active dune on Paren-garenga](#)  
1587 [Sandspit, New Zealand, The Leading Edge, 22, 865–881, 2003.](#)  
1588 [Wang, P., Hu, Z., Zhao, Y., and Li, X. Experimental study of soil compaction effects](#)  
1589 [on GPR signals, Journal of Applied Geophysics, 126m 128-137, 2016.](#)  
1590 Wei, T. Package 'corrplot'-Visualization of a correlation matrix. v0.60. cran. rproject.  
1591 org, 2012.  
1592 Werner, C., Schmid, M., Ehlers, T.A., Fuentes-Espoz, J.P., Steinkamp, J., Forrest,  
1593 M., Liakka, J., Maldonado, A., and Hickler, T. Effect of changing vegetation and  
1594 precipitation on denudation - Part1; Predicted vegetation composition and cover  
1595 over the last 21 thousand years along the Coastal Cordillera of Chile, Earth  
1596 Surface Dynamics, 6, 829-858, <https://doi.org/10.5194/esurf-6-829-2018>, 2018.  
1597 Wold, S., Esbensen, K., and Geladi, P. Principal component analysis,  
1598 Chemometrics and intelligent laboratory systems, 2, 37-52, 1987.  
1599 [Yoder, R.E., Freeland, R.S., Ammons, J.T., and Leonard, L.L. Mapping agricultural](#)  
1600 [fields with GPR and EMI to identify offsite movement of agrochemicals, Journal](#)  
1601 [of Applied Geophysics, 47, 3-4, 251-259, 2001.](#)  
1602 Zhang, J., Lin, H., and Doolittle, J. Soil layering and preferential flow impacts on  
1603 seasonal changes of GPR signals in two contrasting soils. [Geoderma](#), 213,  
1604 560-569, 2014.  
1605 [Zhang, X., Dao, L., Zhang, C., Morrison, L., Hong, B., Zhang H., and Gan, Y.](#)  
1606 [Mapping the spatial distribution of soil depth in a grassland ecosystem with the](#)  
1607 [aid of ground penetrating radar and GIS \(Northwestern Sichuan, China\),](#)  
1608 [Grassland Science, 64, 4, 217-225, 2018.](#)  
1609  
1610  
1611

Formatted: Line spacing: single

Formatted: Line spacing: single

Deleted: geoderman

Deleted: ¶

Formatted: Line spacing: single

Formatted: Font colour: Text 1

1614 **Figure captions**

1615 Fig. 1:

1616 Digital elevation model (Data source: GTOPO30) for the Chilean Coastal Cordillera  
1617 and the Central Andes showing the four investigated study areas (from [north](#) to  
1618 [south](#)): Pan de Azúcar (~26° S); Santa Gracia (~30° S); La Campana (~33° S); and  
1619 Nahuelbuta (~38° S).

Deleted: N

Deleted: S

1620

1621 Fig. 2:

1622 Satellite images (Data source: Google Earth©) of the four study areas from N to S  
1623 in latitude: A) Pan de Azúcar; B) Santa Gracia; C) La Campana; and D) Nahuelbuta.  
1624 Red stars indicate the pedon positions whereas the blue lines represent the  
1625 locations of the geophysical investigations.

1626

1627 Fig. 3:

1628 N- and S-facing hillslopes of the four study areas with locations of pedons and  
1629 transects of ground penetrating radar indicated by the red double arrows. [For  
1630 complete characterization and interpretation of the pedons see Fig. 2 in Bernhard  
1631 et al. \(2018\) and Figs 3 to 6 in Oeser et al. \(2018\).](#)

Deleted: soil

Formatted: Indent: Left: -0.01 cm

1632

1633 Fig. 4:

1634 Compilation of physical and chemical investigations with depth at the pedon location  
1635 in the mid-slope position of the S-facing hillslope in Pan de Azúcar. Properties  
1636 shown are: 1) GPR transect and the envelope profile of the 500 MHz measurement;  
1637 2) GPR transect and the envelope profile of the 1000 MHz measurement; 3) Bulk  
1638 density; 4) Grain size distribution of sand, silt, and clay; 5) Loss on ignition LOI; 6)  
1639 Chemical index of alteration CIA; 7) Chemical index of the mass transfer coefficient  
1640 Tau  $\tau$ ; and 8) volumetric strain  $\epsilon_{strain}$ . The black line indicates the boundary between  
1641 the mobile [pedolith](#) and the immobile [saprolite](#) (after Oeser et al., 2018) and the gray  
1642 area with green lines reflects the transition zone from B to C horizon (after Bernhard  
1643 et al., 2018).

Deleted: soil

Deleted: saprolite

1649

1650 Fig. 5:

1651 Primary component analysis PCA of properties for all four pedons in Pan de Azúcar.

1652 A) Scree plot showing the percentage of explained variances and B) Variables -

1653 PCA.

1654

1655 Fig. 6:

1656 Compilation of physical and chemical investigations at the pedon location in the mid-

1657 slope position of the S-facing hillslope in Santa Gracia. Properties shown are listed

1658 in caption of Fig. 4.

1659

1660 Fig. 7:

1661 Primary component analysis PCA of properties for all four pedons in Santa Gracia.

1662

1663 Fig. 8:

1664 Compilation of physical and chemical investigations at the pedon location in the mid-

1665 slope position of the S-facing hillslope in La Campana. Properties shown are listed

1666 in in caption of Fig. 4.

1667

1668 Fig. 9:

1669 Primary component analysis PCA of properties for all four pedons in La Campana.

1670

1671 Fig. 10

1672 Compilation of physical and chemical investigations at the pedon location in the mid-

1673 slope position of the S-facing hillslope in Nahuelbuta. Properties shown are listed

1674 as in caption of Fig. 4. Note that only the 500 MHz signal and envelope profile exist.

1675

1676 Fig. 11:

1677 Primary component analysis PCA of properties for all four pedons in Nahuelbuta.

1678

Deleted: soil

Deleted: soil

Deleted: soil

Deleted: soil

1683 Fig. 12:  
1684 A) 1000 MHz GPR transect and B) envelope for the S-facing hillslope in Pan de  
1685 Azúcar. The hillslope transect spans over ~20 m and includes pedon AZPED60,  
1686 AZPED50, and AZPED40 (black boxes). The potential [pedolith](#) thickness based on  
1687 the envelopes is indicated by stars (in B). The red bar indicates the B to C horizon  
1688 transition as given in Bernhard et al. (2018). Uphill is from left to right. Note that in  
1689 the radar data the air wave and background removal is applied.

Deleted: soil

1690  
1691 Fig. 13:  
1692 1000 MHz GPR signal and envelope for the mid-slope position of the S-facing  
1693 hillslope position in Santa Gracia (SGPED40). The hillslope transect spans over ~20  
1694 m. Interpretation of the radar signal are indicated where possible (stippled lines in A  
1695 and B). The potential [pedolith](#) thickness is indicated based on the envelope profile.  
1696 Uphill is from left to right. Lines and symbols in figures as described in Fig. 12.

Deleted: soil

1697  
1698 Fig. 14:  
1699 500 MHz GPR signal and envelope for the mid-slope position of the S-facing  
1700 hillslope in La Campana (LCPED20). The hillslope transect spans over ~8 m.  
1701 Interpretation of the radar signal are indicated where possible (stippled and black  
1702 lines in A and B). The potential [pedolith](#) thickness is indicated based on the envelope  
1703 profile. Uphill is from left to right. Lines and symbols in figures as described in Fig.  
1704 12.

Deleted: soil

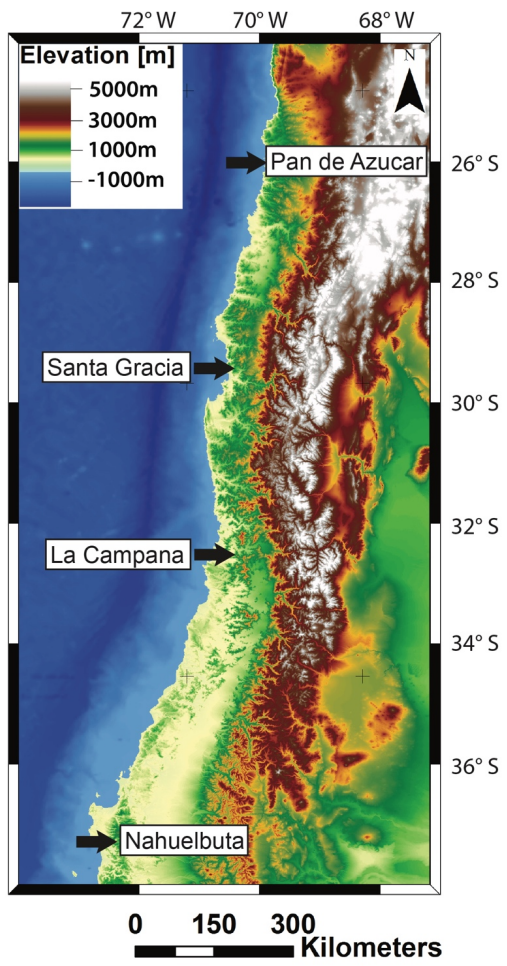
1705  
1706 Fig. 15:  
1707 500 MHz GPR signal and envelope for the mid-slope position of the S-facing  
1708 hillslope in Nahuelbuta (NAPED20). The hillslope transect spans over ~20 m.  
1709 Interpretation of the radar signal are indicated where possible (stippled lines in A  
1710 and B). The potential [pedolith](#) thickness is indicated based on the envelope profile.  
1711 Uphill is from left to right. Lines and symbols in figures as described in Fig. 12.

Deleted: soil

1712

1717

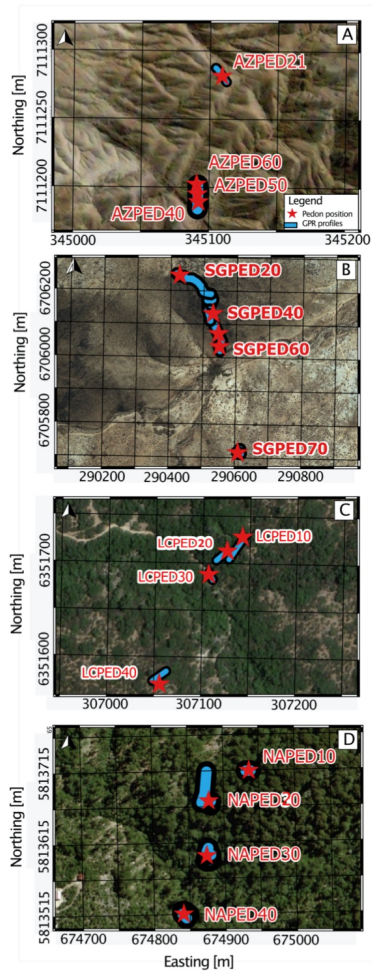
1718 Fig. 1:



1719  
1720

Formatted

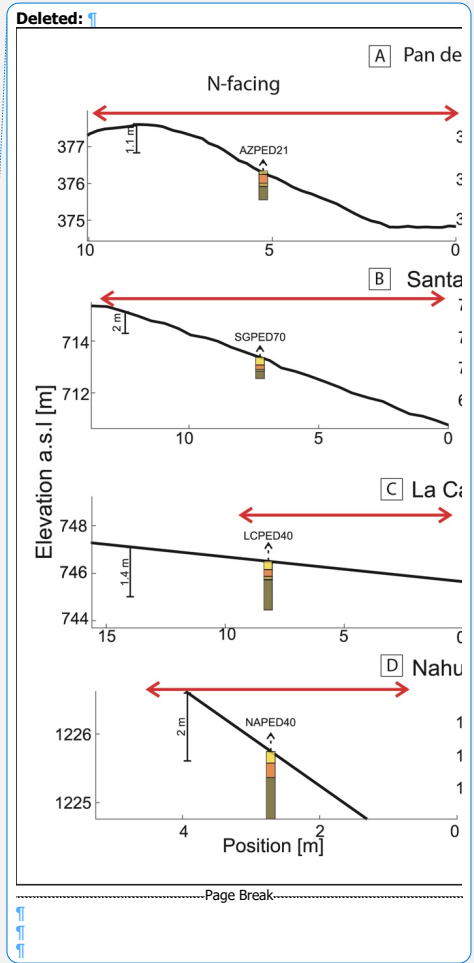
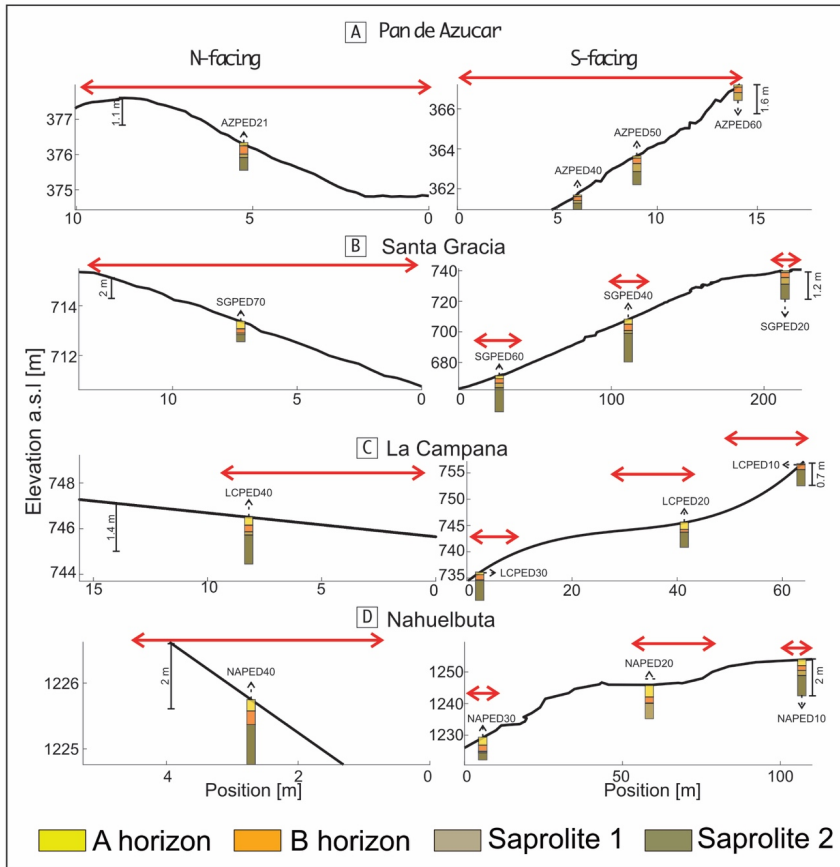
1721 Fig. 2:



Formatted

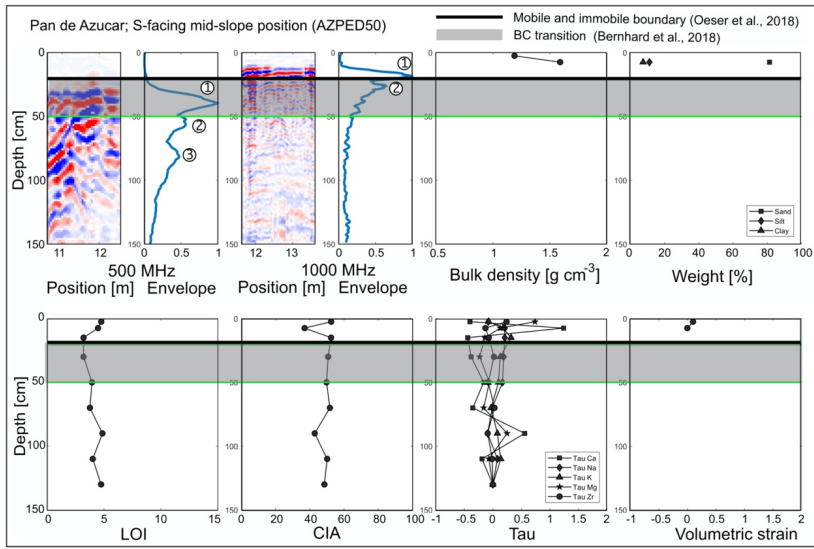
1722

1723 Fig. 3:



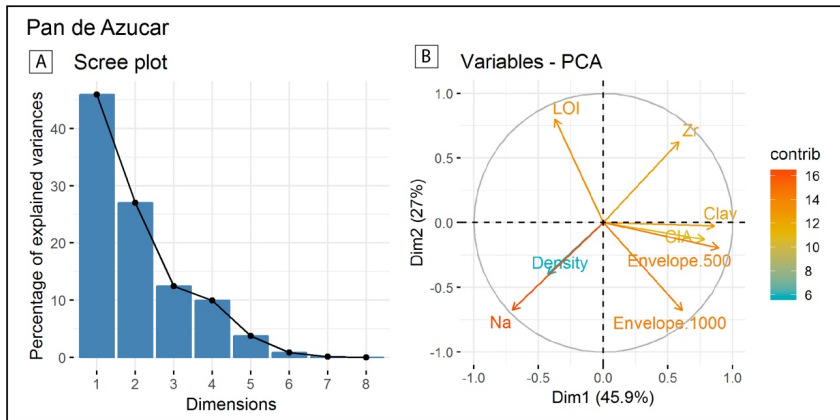
1724  
1725

1732 Fig. 4:

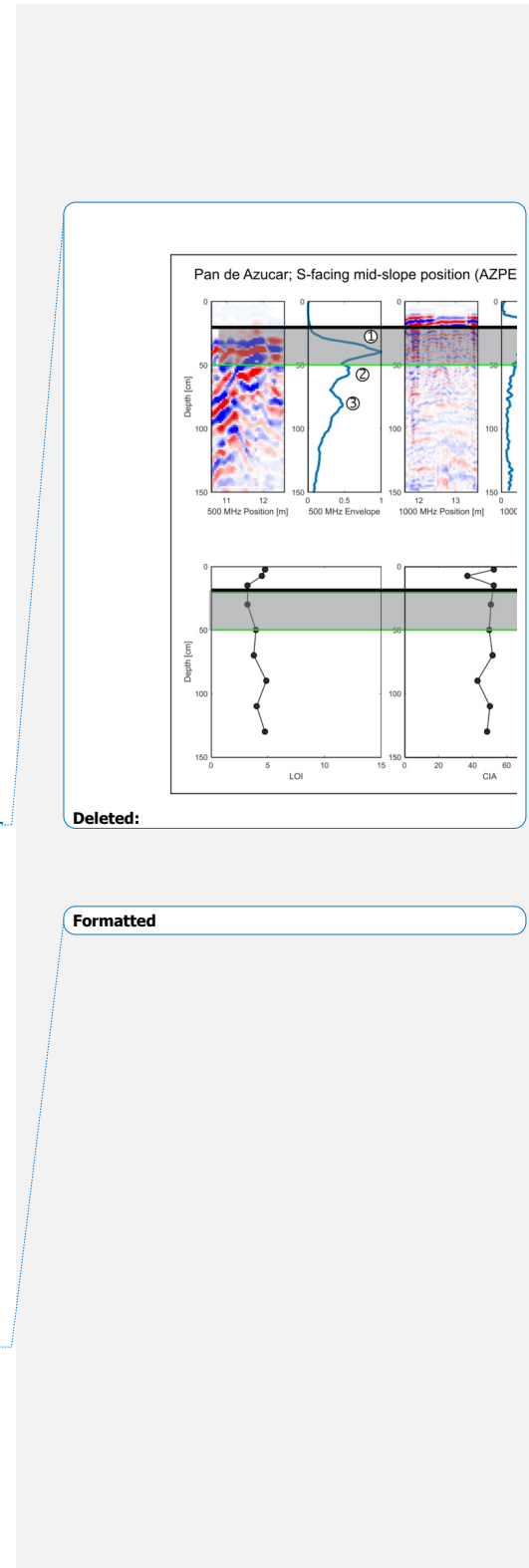


1733  
1734  
1735  
1736

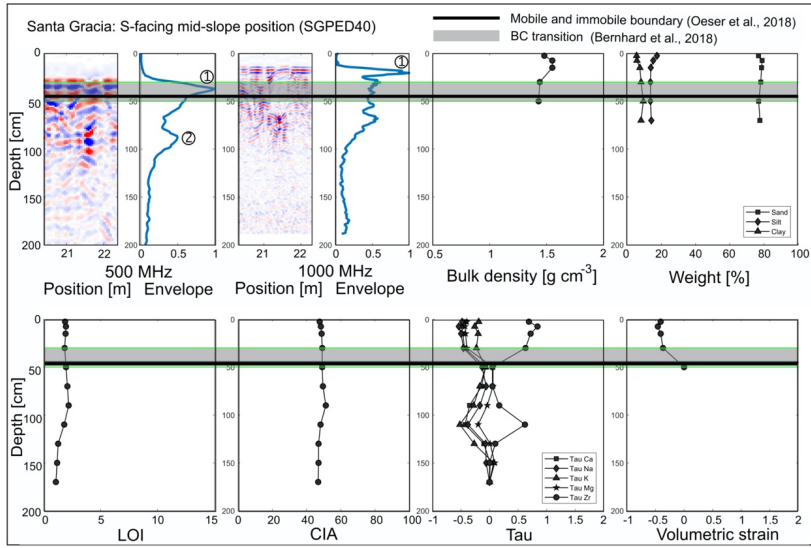
Fig. 5:



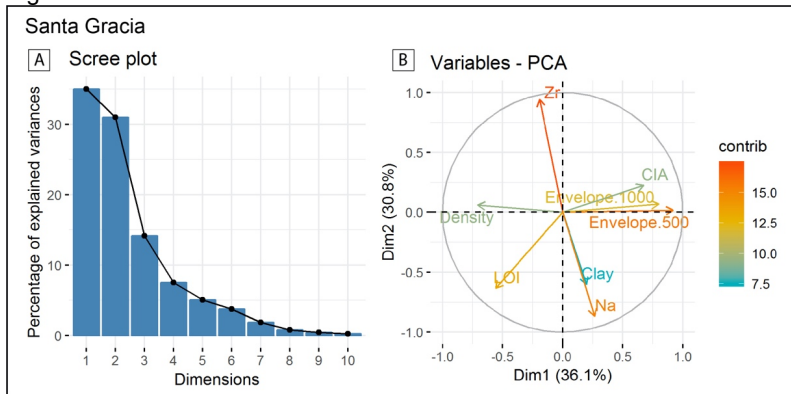
1737  
1738  
1739



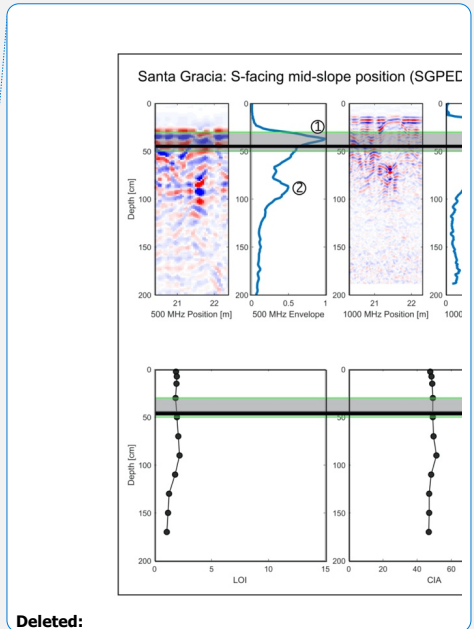
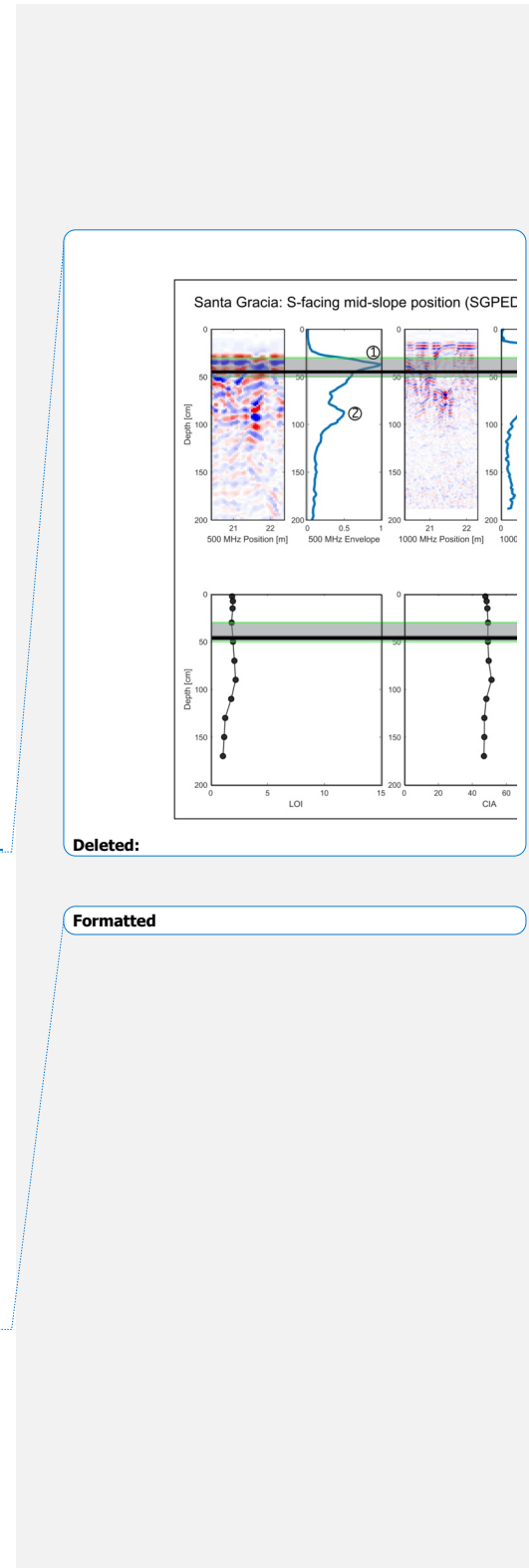
1741  
1742 Fig. 6:



1743  
1744  
1745 Fig. 7:



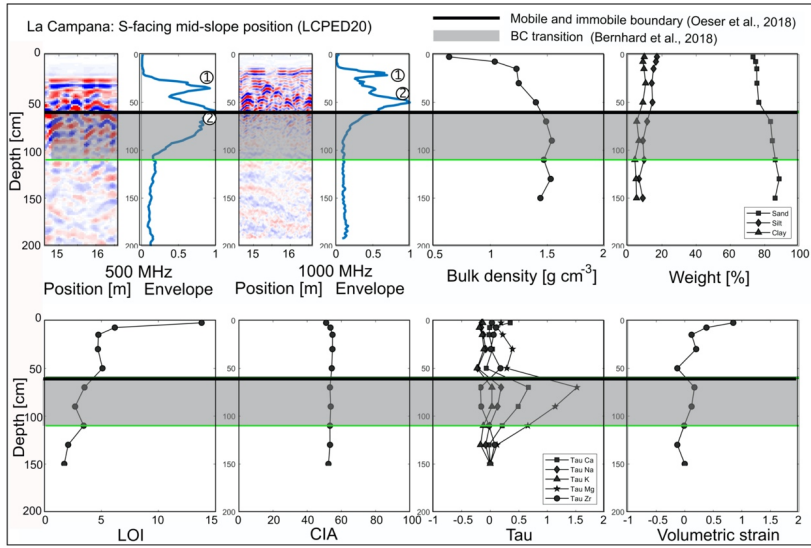
1746  
1747  
1748



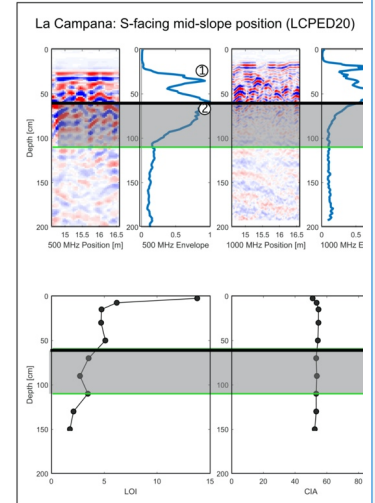
Formatted

1750  
1751

Fig. 8:



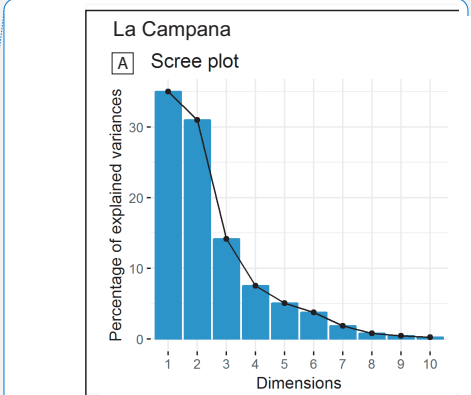
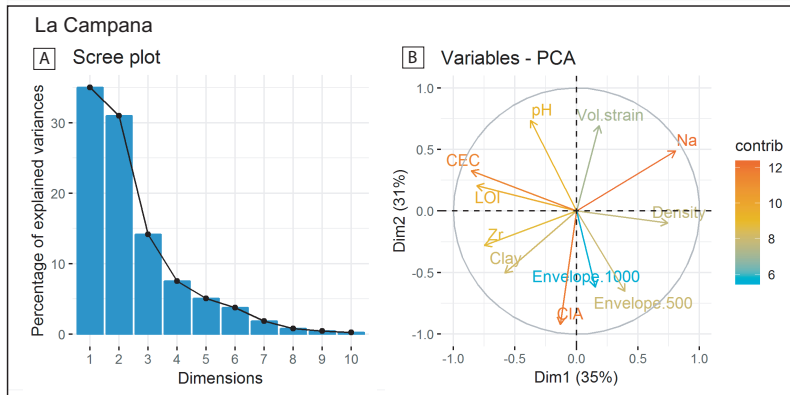
Deleted:



Deleted:

1752  
1753  
1754  
1755

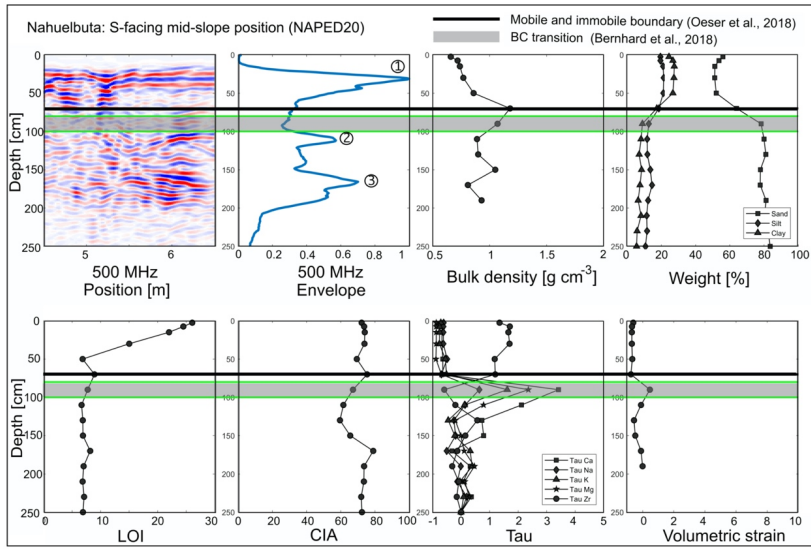
Fig. 9:



Deleted:

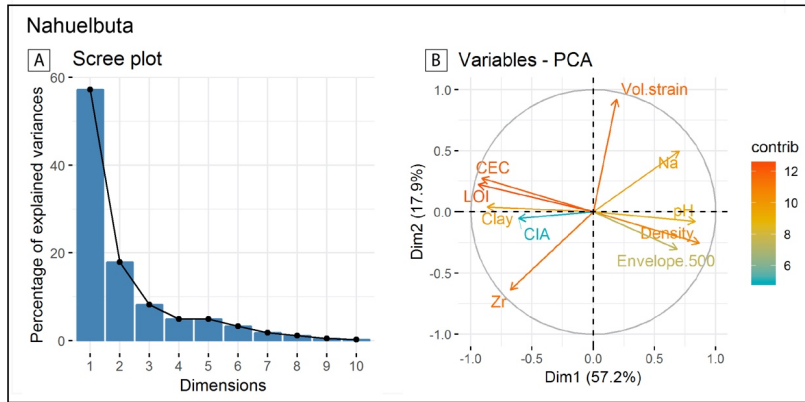
1756  
1757

1762 Fig. 10:

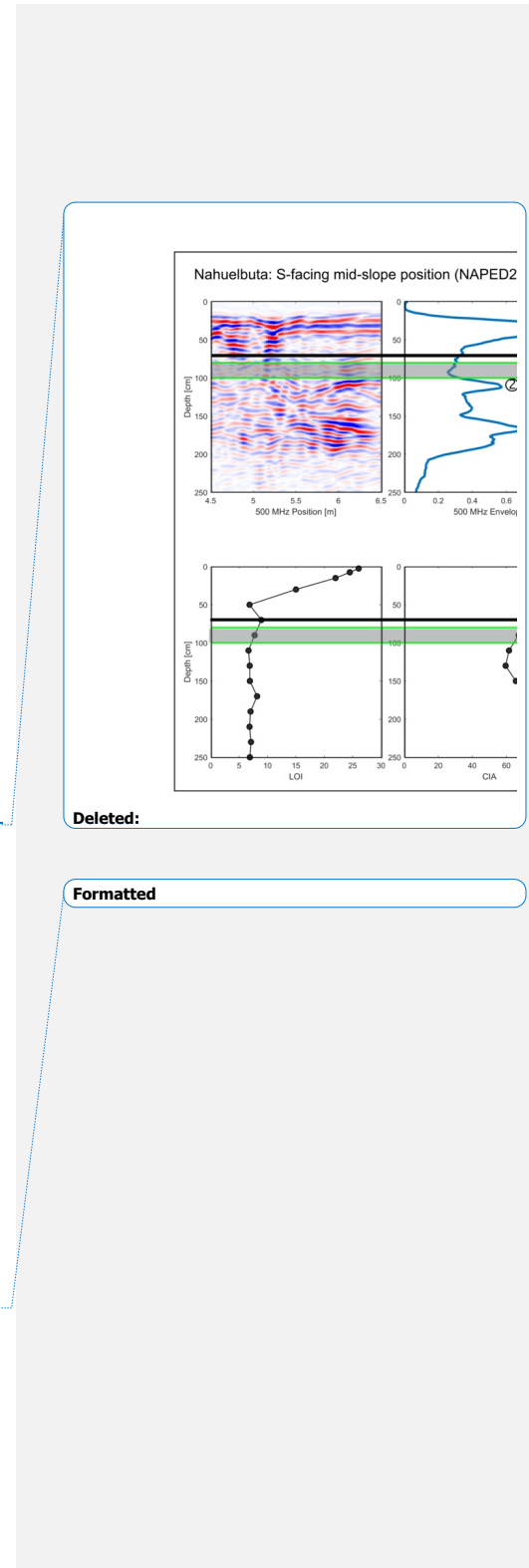


1763  
1764  
1765

Fig. 11:



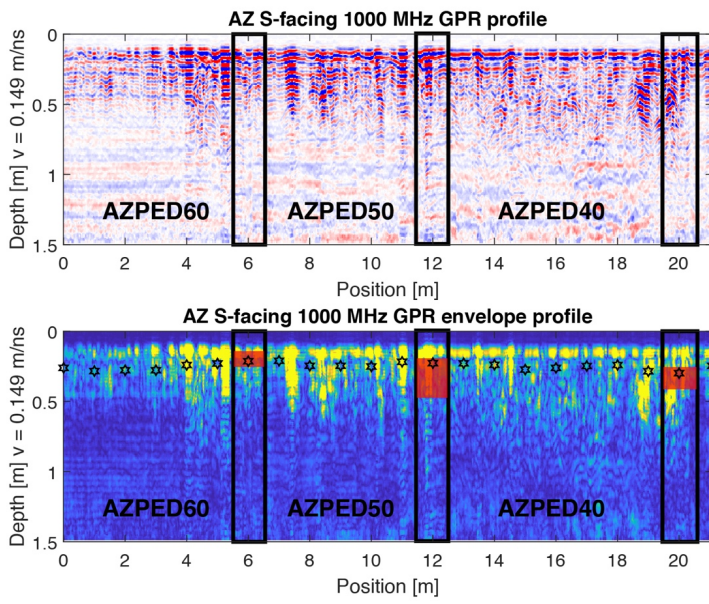
1766  
1767  
1768  
1769



Deleted:

Formatted

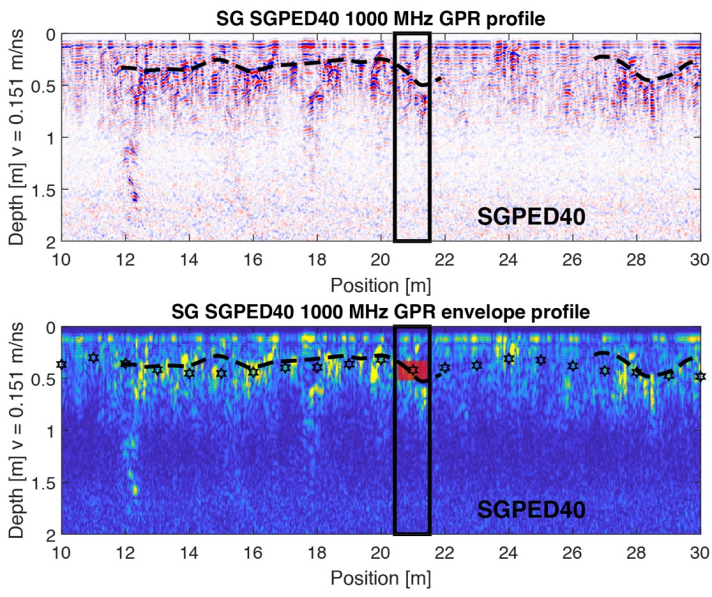
1771 Fig. 12:  
1772



1773  
1774  
1775

Formatted

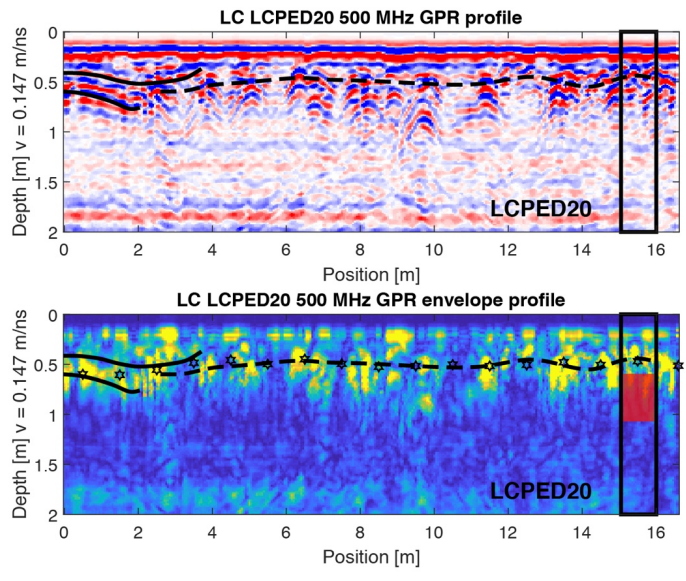
1776 Fig. 13:



Formatted

1777  
1778

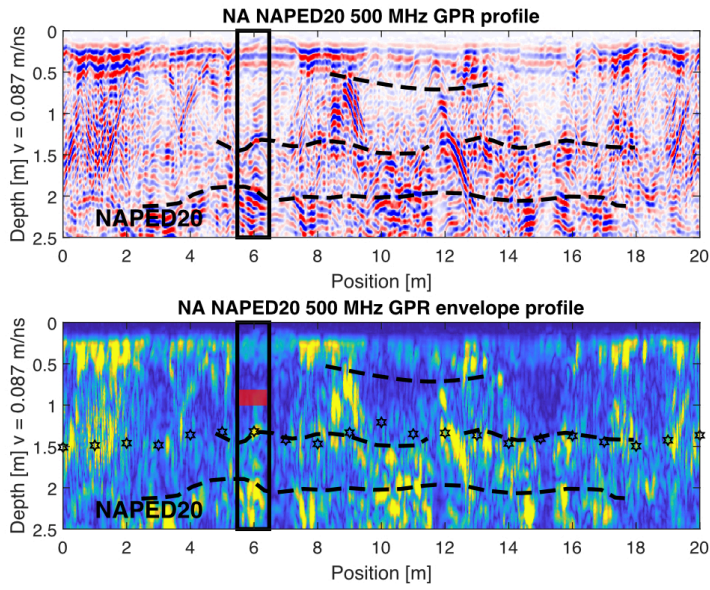
1779 Fig. 14:  
1780



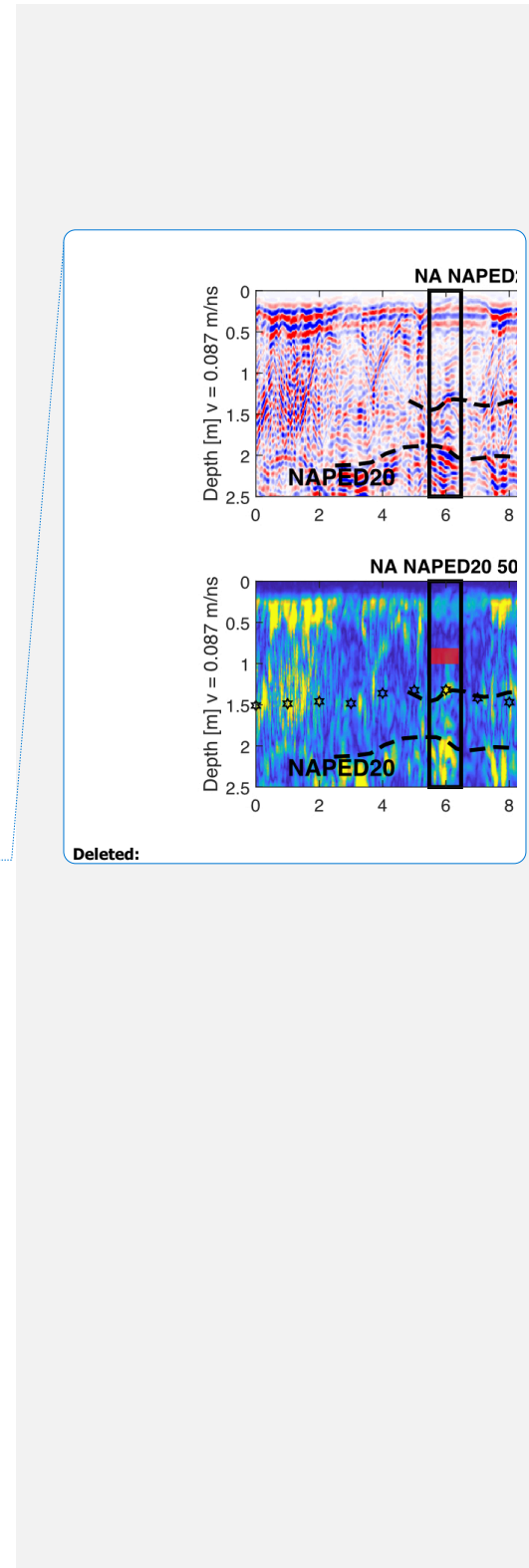
1781  
1782  
1783

Formatted

1784 Fig. 15:  
1785



1786  
1787



1789  
1790  
1791

Table 1:

Table 1: Data compilation for pedons in the investigated four study areas in the Chilean Coastal Cordillera

Pedon	Location		Altitude m	Position	Aspect °	Slope °	BC-horizon transition <sup>(1)</sup> cm	Field observations			GPR point depth <sup>(5)</sup>		GPR transect depth <sup>(6)</sup>	
	'S	'W						Mobile/immob. <sup>(2)</sup> cm	Mobile/immob. <sup>(3)</sup> cm	GPR <sup>(4)</sup> cm	500 MHz cm	1000 MHz cm	500 MHz cm	1000 MHz cm
<b>Pan de Azucar</b>														
AZPED60	26.11012	70.54922	343	top	60	5	14-26		22	30-55 (?)	40	20/25/45		
AZPED50	26.11027	70.54922	333	mid	0	40	20-50	20	20-55	40/50/70	20/25/35/45			
AZPED40	26.11024	70.54921	326	toe	0	33	23-40	25	20-40	40/55	20/30			
AZPED21	26.10936	70.54907	342	mid	180	25	20-30	20	20-30-45	37/55/75	20/30/45/55	40 ± 2	28 ± 7	
<b>Santa Gracia</b>														
SGPED20	29.75636	71.16721	718	top	240	5	20-30		30	30	40	20/30/40/50	37 ± 5	34 ± 3
SGPED40	29.75738	71.16635	682	mid	0	25	30-50	50	45	60	45/10/30/40/55/65	40 ± 7	36 ± 5	
SGPED60	29.75826	71.16615	638	toe	0	20	40-60		55	-	37/50	39 ± 7	35 ± 6	
SGPED70	29.76120	71.16559	690	mid	180	15	25	35	35	NA	40	20/30	35 ± 3	28 ± 2
<b>La Campana</b>														
LCPED10	32.95581	71.06332	734	top	60	7	34		45	40/50	35/50/70/10/30/35/50/65	55 ± 6	44 ± 5	
LCPED20	32.95588	71.06355	718	mid	0	23	60-110	60	60	50/60	35/60/70	59 ± 6	45 ± 4	
LCPED30	32.95615	71.06380	708	toe	60	35	34-55		55	45/50	35/70	50 ± 9	41 ± 4	
LCPED40	32.95720	71.06425	724	mid	120	12	36-103	35	35	-	35/65	20/30/40	56 ± 6	47 ± 6
<b>Nahuelbuta</b>														
NAPED10	37.80735	73.01285	1248	top	60	5	50-75		70	70/75	35/45/120	82 ± 15		
NAPED20	37.80770	73.01357	1239	mid	60	15	80-100	95	70	75/95	35/110/170	101 ± 8		
NAPED30	37.80838	73.01345	1228	toe	0	20	63-85		90	-	5/90/120/140	96 ± 6		
NAPED40	37.80904	73.01380	1200	mid	180	13	65-90	70	60	40/50	40/60/120	95 ± 11		

<sup>(1)</sup> Depth of BC-horizon transition from Bernhard et al., 2018  
<sup>(2)</sup> Depth of mobile pedolith from Schaller et al., 2018  
<sup>(3)</sup> Depth of mobile pedolith from Oeser et al., 2018  
<sup>(4)</sup> Depth based on data from Dal Bo et al., 2019  
<sup>(5)</sup> Depth based on single point GPR envelopes (This study)  
<sup>(6)</sup> Average depth based on envelopes from GPR transect data (This study)

Table 1: Overview of physical, chemical, and geophysical properties determined in the four different study areas

Property	Abbreviation	Units
Soil bulk density	ρ <sub>b</sub>	g/cm <sup>3</sup>
Grain size distribution	GSD	%
Potential hydrogene	pH	
Cation exchange capacity	CEC	cmol <sub>c</sub> /kg
Loss on ignition	LOI	%
Chemical index of alteration	CIA	
Mass transfer coefficient	τ	m/s
Volumetric strain	ε <sub>strain</sub>	
Electric permittivity	ε <sub>r</sub>	
Electrical conductivity	σ	mS/m

Deleted:

1792  
1793  
1794  
1795  
1796  
1797  
1798  
1799  
1800

Table 2:

Table 2: Overview of physical, chemical, and geophysical properties determined in the four different study areas

Property	Abbreviation	Units	Meaning	Reference
Pedolith bulk density	ρ <sub>b</sub>	g/cm <sup>3</sup>	Weight of unit volume	Bernhard et al., 2018
Grain size distribution	GSD	%	Weight percent of different grain sizes smaller than 2 mm	Bernhard et al., 2018
Potential hydrogene	pH		Acid and base properties	Bernhard et al., 2018
Cation exchange capacity	CEC	cmol <sub>c</sub> /kg	Soil ability to hold positively charged ions	Bernhard et al., 2018
Loss on ignition	LOI	%	Loss of volatiles due to excessiv heating	Oeser et al., 2018
Chemical index of alteration	CIA		Degree of weathering	Oeser et al., 2018
Mass transfer coefficient	τ	m/s	Chemical gain or loss	Oeser et al., 2018
Volumetric strain	ε <sub>strain</sub>		Volumetric gain or loss	Oeser et al., 2018
Electric permittivity	ε <sub>r</sub>		Structural changes, porosity/soil water content	Dal Bo et al., 2019; This study
Electrical conductivity	σ	mS/m	Clay, salinity	Dal Bo et al., 2019; This study

Table 2: Data compilation for pedons in the investigated four study areas in the Chilean Coastal Cordillera

Soil profile	Location		Altitude m	Position	Aspect °	Slope °	BC-horizon cm
	'S	'W					
<b>Pan de Azucar</b>							
AZPED60	26.11012	70.54922	343	top	60	5	
AZPED50	26.11027	70.54922	333	mid	0	40	
AZPED40	26.11024	70.54921	326	toe	0	33	
AZPED21	26.10936	70.54907	342	mid	180	25	
<b>Santa Gracia</b>							
SGPED20	29.75636	71.16721	718	top	240	5	
SGPED40	29.75738	71.16635	682	mid	0	25	
SGPED60	29.75826	71.16615	638	toe	0	20	
SGPED70	29.76120	71.16559	690	mid	180	15	
<b>La Campana</b>							
LCPED10	32.95581	71.06332	734	top	60	7	
LCPED20	32.95588	71.06355	718	mid	0	23	
LCPED30	32.95615	71.06380	708	toe	60	35	
LCPED40	32.95720	71.06425	724	mid	120	12	
<b>Nahuelbuta</b>							
NAPED10	37.80735	73.01285	1248	top	60	5	
NAPED20	37.80770	73.01357	1239	mid	60	15	
NAPED30	37.80838	73.01345	1228	toe	0	20	
NAPED40	37.80904	73.01380	1200	mid	180	13	

<sup>(1)</sup> Depth of BC-horizon transition from Bernhard et al., 2018  
<sup>(2)</sup> Depth of mobile layer from Schaller et al., 2018  
<sup>(3)</sup> Depth of mobile layer from Oeser et al., 2018  
<sup>(4)</sup> Depth based on data from Dal Bo et al., 2019  
<sup>(5)</sup> Depth based on single point GPR envelopes (This study)  
<sup>(6)</sup> Average depth based on envelopes from GPR transect data (This study)

Deleted:

1801  
1802  
1803  
1804  
1805  
1806

1812  
 1813  
 1814  
 1815  
 1816

[Table 3:](#)

Table 3: Correlation coefficients R of 1000 and 500 MHz GPR envelope with derivatives of physical and chemical properties for each study area										
Study area		Bulk density	Clay content	pH	CEC	LOI	CIA	Tau		Vol. strain
								Na	Zr	
1000 MHz										
Pan de Azucar	GPR	0.05	0.54				-0.1	-0.2	-0.1	-0.15
Santa Gracia	GPR	-0.03	0.3				0.14	0.33	-0.16	0.1
La Campana	GPR	-0.04	0.19	-0.34	-0.35	-0.19	0.43	-0.12	0.07	-0.18
Nahuelbuta	GPR									
Earth Shape	GPR	0.01	0.25	-0.15	-0.24	0.02	0	-0.14	0.01	
500 MHz										
Pan de Azucar	GPR	-0.29	0.17				-0.27	0.28	0.16	-0.07
Santa Gracia	GPR	-0.39	0.26				-0.02	0.26	-0.08	0.02
La Campana	GPR	0.2	0.22	-0.57	-0.39	-0.26	0.56	0.09	-0.26	-0.12
Nahuelbuta	GPR	0.74	-0.37	0.46	-0.53	-0.60	-0.24	0.21	-0.28	-0.01
Earth Shape	GPR	-0.16	-0.02	-0.39	-0.45	-0.03	0.45	0.11	-0.15	

1817

<b>Page 10: [1] Deleted</b>	<b>Microsoft Office User</b>	<b>23/10/2020 14:46:00</b>
-----------------------------	------------------------------	----------------------------

▼

<b>Page 10: [2] Deleted</b>	<b>Microsoft Office User</b>	<b>23/10/2020 14:46:00</b>
-----------------------------	------------------------------	----------------------------

▼

<b>Page 10: [3] Deleted</b>	<b>Microsoft Office User</b>	<b>23/10/2020 14:46:00</b>
-----------------------------	------------------------------	----------------------------

▼

<b>Page 22: [4] Deleted</b>	<b>Microsoft Office User</b>	<b>23/10/2020 14:46:00</b>
-----------------------------	------------------------------	----------------------------

▼

<b>Page 22: [5] Deleted</b>	<b>Microsoft Office User</b>	<b>23/10/2020 14:46:00</b>
-----------------------------	------------------------------	----------------------------

▼